



NASA Public Access

Author manuscript

J Hydrol (Amst). Author manuscript; available in PMC 2019 September 01.

Published in final edited form as:

J Hydrol (Amst). 2018 September ; 564: 559–573. doi:10.1016/j.jhydrol.2018.07.030.

Satellite observations and modeling to understand the Lower Mekong River basin streamflow variability

Ibrahim Nourein Mohammed*,

Science Applications International Corporation, Hydrological Sciences Laboratory, NASA Goddard Space Flight Center, Mail Code 617.0, Greenbelt, MD 20771, USA

John D. Bolten,

Hydrological Sciences Laboratory, NASA Goddard Space Flight Center, Mail Code 617, Greenbelt, MD 20771, USA

Raghavan Srinivasan, and

Spatial Sciences Laboratory, Department of Ecosystem Science and Management, Texas A&M University, College Station, TX 77843, USA

Venkat Lakshmi

School of Earth Ocean and Environment, University of South Carolina, Columbia, SC 29208, USA

Abstract

In this work, we have used the Soil & Water Assessment Tool (SWAT) to examine streamflow variability of the Lower Mekong River Basin (LMRB) associated with changes in the Upper Mekong River Basin (UMRB) inflows. Two hypothetical experiments were formulated and evaluated for the LMRB, where we conducted runoff simulations with multiple inflow changes that include upstream runoff yield increase and decrease scenarios. Streamflow variability of the LMRB was quantified by two streamflow metrics that explain flow variability and predictability, and high flow disturbance. The model experiments were performed for the Lower Mekong River Basin with identical climate, soil, and other watershed characteristics data. Remote sensing precipitation (Tropical Rainfall Measurement Mission, TRMM, and Global Precipitation Measurement mission, GPM), meteorological data as well as spatial data that include a digital elevation model, newly developed soil information (Harmonized World Soil Database, HWSD), and land use and land cover were processed as input to the LMRB model simulations. Observed daily streamflow data along the Lower Mekong River from Chiang Sean, Thailand to Kratie, Cambodia were used for calibration and validation. Our work results suggest that the Lower Mekong River streamflow is highly variable and has a low predictability (Colwell index of about 32%). We found that releasing more water from upstream Mekong during rainfall months by 30% would result in a reduction in the Lower Mekong streamflow predictability by about 21%. This reduction in predictability is mainly attributed to a decrease in the Contingency index. Our work

*Corresponding author: Tel: +1-301-614-6537, ibrahim.Mohammed@nasa.gov.

Appendix B. Supplementary data

Supplementary data associated with this article can be found, in the online version, at <https://doi.org/10.1016/j.jhydrol.2018.07.030>.

The supplementary data include compressed keyhole markup language file (KMZ) that contains geographic annotations for the various layers described in this article.

shows that the ability to predict floods/droughts at the Lower Mekong River would be reduced if there is any anticipated change (i.e., increase/decrease) from UMRB releases. Our results also show that releasing more flows from the upstream Mekong would also affect flood duration and the frequency of flood occurrences downstream. The results of this work thus help to quantify the sensitivity of streamflow variability at the Lower Mekong River Basin to upstream anthropogenic changes.

Keywords

Mekong River; Streamflow variability; Streamflow predictability; Remote sensing; SWAT; Flooding

1. Introduction

Freshwater availability is necessary to promote economic growth through agriculture, fisheries, transport, environmental health, and social equity (Haddeland et al., 2006; Mekong River Commission, 2017; Milly et al., 2005; Veilleux and Anderson, 2016; Wang, 2017; Ziv et al., 2012). Water resources are becoming increasingly limited in availability across the globe. Water shortages may be simplistically attributed to droughts, regulatory cutbacks in deliveries, and demands that outpace new infrastructure and expansion of supply (Grafton et al., 2013; Räsänen et al., 2017; Zhang et al., 2014). Water resources planning efforts are complicated by uncertainty stemming from patterns of economic growth, changes in water use patterns, land use change, and climate change (DeFries and Eshleman, 2004; Dudgeon et al., 2006; Gleick, 2000; Grafton et al., 2013; Jacobs, 2002; Milly et al., 2008; Vörösmarty et al., 2010; Winemiller et al., 2016). While these processes directly increase demands, or decrease supply, research has demonstrated that there are complex processes and dynamic feedbacks among physical processes, biological, biochemical and human-mediated processes that determine change in the water system (Ceola et al., 2014; Heistermann, 2017; Hester and Doyle, 2011; Montanari et al., 2013; Mosley, 2015).

Agriculture is one of the most important aspects to the society and economy and has an enormous impact on the well-being of the countries in the Lower Mekong River Basin (LMRB) such as Vietnam, Thailand, Laos People's Democratic Republic (PDR) and Cambodia (Mainuddin and Kirby, 2009; Mekong River Commission, 2009b). The Mekong River Basin has experienced large variations in precipitation and hence agricultural productivity (Mainuddin and Kirby, 2009). In order to understand these variations over large spatial scales and long-time periods, a better understanding of (i.e., observation and prediction) the hydrologic cycle is necessary – hence use of satellite data and models is warranted (Hoang et al., 2016; Kite, 2001; Lakshmi, 2004; Lyon et al., 2017; Piman et al., 2013b; Wang et al., 2016; Wild and Loucks, 2014).

The seasonal variations in the Mekong River's flow typically follow a dry season (December to May) and a wet season or a flood season (July to October). The Mekong River streamflow regime changes have been studied in multiple studies (Cochrane et al., 2014; Delgado et al., 2010; Kummur and Sarkkula, 2008; Li et al., 2017; Lu Xi Xi and Grundy-Warr, 2008; Mekong River Commission, 2009a; Piman et al., 2013a; Räsänen et al., 2012; Räsänen et al.,

2017; Thanh et al., 2015). These studies summarized the observed Mekong River streamflow regime change as streamflow reduction during wet seasons and streamflow increase in dry seasons. Studies cited above have tried to discern the causes for such alterations in the Mekong River streamflow regimes. It has been found that the main causes for streamflow alterations in the Mekong River were attributed to human activities and climate change effects (Hoang et al., 2016; Wang et al., 2017a). Studies on flow regime characterization have been examined via metrics that describe the magnitude, frequency, duration, timing and rate of change for streamflow (Poff, 1996; Poff et al., 1997). Human activities occurring in the Upper Mekong River Basin (UMRB) altering the Mekong flows have recognizable impacts on Lower Mekong streamflow regimes as seen in aquatic ecosystems species, nutrient delivery, water temperatures, riparian livelihoods, sediment movement, and floodplain interactions. Recent studies on the Lower Mekong River highlighted the critical need for specifying and implementing flow regimes to address trade-offs between socioeconomic activities (e.g., fishery), ecological needs, and energy security (Poff and Olden, 2017; Sabo et al., 2017).

This work has integrated multiple satellite-based earth observation systems and spatial data with the Soil & Water Assessment Tool (SWAT) hydrologic model employed in the Mekong Basin region to explore water availability, based on both hydrologic flows and total water demands/use using and enhanced remotely sensed products. The scarcity and the incompleteness of many gauge data observations make it imperative to use remote sensing data in modeling the LMRB. From this work, a comprehensive suite of hydrologic data products has been developed and used to improve water accounting and floodplain management using the hydrological cycle variables such as air temperature, evapotranspiration, and precipitation in the LMRB. The main objective of this work is the better understanding of the hydrological cycle of the LMRB, and the floodplain management over the basin. We explore the streamflow variability of the Lower Mekong River by examining the impacts associated with changes in the UMRB inflow. The UMRB inflow to the Lower Mekong changes are generally due to reservoir construction for hydropower development. Overall, our work aims to assess the value-added information of simulating hydrological processes in the LMRB by using a hydrological model (SWAT) with climatological forcing data of satellite-based earth observation as an alternative to scarce in-situ data.

2. Methods

2.1. Study Site

The Mekong River originates in the high altitude of the Tibetan Plateau in China and flows south through five countries (Myanmar, Laos PDR, Thailand, Cambodia, and Vietnam) ending in a large delta before exiting to the South China Sea. The Mekong River Basin is divided into the Upper and the Lower basins. The Lower Mekong River Basin begins when the Mekong River leaves the Chinese province of Yunnan and enters the Golden Triangle where the country borders of Thailand, Laos PDR, China and Myanmar come together (Figure 1).

2.2. Spatial Data

A digital elevation model (DEM) with 1 arc-sec grid resolution for the study area was obtained from the Advanced Spaceborne Thermal Emission and Reflection Radiometer (ASTER) Global Digital Elevation Model (<https://doi.org/10.5067/ASTER/ASTGTM.002>). The DEM map with 90-meter resolution was used to derive slope and aspect grids for the LMRB model input. The slope class of 2%—8% covers about 40% of the watershed area.

The study area soil information data was obtained from the Harmonized World Soil Database, HWSO (FAO et al., 2012). The LMRB soil texture is mainly sandy clay loam and covers approximately 42% of the basin.

The Land Use/Land Cover (LULC) data was obtained from a 2010 LULC map at a spatial resolution of a 0.25 kilometer for the Lower Mekong Basin using 2010 Moderate Resolution Imaging Spectroradiometer (MODIS) monthly normalized difference vegetation index (NDVI) data as the primary data source (Spruce et al., 2017). The study watershed LULC areas are mainly forest and agricultural lands. The rice crop is farmed on about 26% of the watershed area, while forest land covers constitute about 30% of the watershed area (Spruce et al., 2017).

2.3. Meteorological Data

Recent works have evaluated the accuracy of satellite-based precipitation in the Mekong River Basin and found that satellite-based precipitation advances hydrological studies in the Mekong region (He et al., 2017; Wang et al., 2017b). For this work, daily cumulative precipitation data was obtained from the Global Precipitation Measurement mission (GPM) and the Tropical Rainfall Measuring Mission (TRMM) remote sensing data and used as inputs for the LMRB model. The Integrated Multi-Satellite Retrievals for GPM (IMERG) dataset used for this work was the GPM_3IMERGDF (<https://pmm.nasa.gov/data-access/downloads/gpm>). Since IMERG data products are only available from 12 March 2014 to present, then we used the TRMM rainfall data (3B42RT) for time periods earlier than 12-March-2014. A nearest neighbor methodology was used in filling the IMERG data points with the TRMM data points as an approximation during the 01 March 2000 to 11 March 2014 time period, because TRMM and IMERG data do not have the same spatial resolution (i.e., 0.25 and 0.1 degree respectively).

Minimum and maximum daily air temperature data was calculated from air temperature record obtained from the Global Land Data Assimilation System (GLDAS) simulation data products (Rodell et al., 2004). For this work, we used the GLDAS_NOAH025_3H.2.1 data products retrieved from <https://disc.gsfc.nasa.gov/>. Wind speed, relative humidity, and solar radiation data needed for our modeling work were estimated using the global reanalysis weather data from the National Centers for Environmental Prediction (NCEP) <http://www.ncep.noaa.gov/>, and the Climate Forecast System Reanalysis (CFSR). Aggregated weighted average annual precipitation, and minimum and maximum air temperature time series for the LMRB are shown in Figure 2. A tool (*nasaaccess*) has been developed and presented in Appendix A.2 to access and process remote sensing data obtained from various NASA servers needed for setting up SWAT model or any other rainfall/runoff model.

2.4. Flow Regime Metrics

In this paper, we examine two streamflow classes and how they change with the UMRB developments at various sites along the LMRB. The streamflow classes studied in this work are flow variability and predictability, and high flow disturbance. A summary of the streamflow regime metrics used to assess UMRB flow change impacts along the LMRB is listed in Table 1. We used the Mann Kendall trend analysis (Helsel and Hirsch, 2002) for trends analyses in flow regime data. Flow variability and predictability streamflow metrics used in this work include a coefficient of variation (*DAYCV*) variable, flow reversals variable (*FLOWREV*), and three flow variables defining the Colwell index which are Predictability (*P*), Constancy (*C*) and Contingency (*M*) (Colwell, 1974). High flow disturbance streamflow metrics used in this work include a flood duration (*FLDDUR*) variable, and a seven-day maximum flow (*7QMAX*) variable. Further details on streamflow classes used are discussed in Appendix A.3.

Streamflow data for this work was obtained from the Mekong River Commission (MRC, www.mrcmekong.org). Updated streamflow data was interpolated from recent observed level data obtained from the Asian Preparedness Disaster Center (*ADPC, personal communication*).

For this work, we used the rescaled range analysis (*R/S*) to calculate the *Hurst* (1951) exponent. *Hurst* (1951) observed that the difference between largest surplus and the greatest deficit gives the capacity that a reservoir must have to maintain a constant release equal to the mean of the river without overflows or deficits during the record period years (*n*). This transitory behavior is widely known as the *Hurst* phenomenon. *Kottegoda and Rosso* (1997) summarize the rescaled range analysis as:

$$\frac{R^*(n)}{s(n)} = cn^H \quad (1)$$

where, $s(n)$ is the standard deviation of the discharge sample of n values, c is a constant equal to $(\pi/2)^{0.5}$, H is the *Hurst* coefficient, $R^*(n)$ is the adjusted range difference between maximum D_n^+ and minimum D_n^- of the accumulated departures from the discharge mean, \bar{X}_n . $R^*(n)$ is explained as:

$$R^*(n) = \max_{1 \leq i \leq n} \left(\sum_{j=1}^i X_j - i\bar{X}_n \right) - \min_{1 \leq i \leq n} \left(\sum_{j=1}^i X_j - i\bar{X}_n \right) = D_n^+ - |D_n^-| \quad (2)$$

2.5. Hydrological Model – SWAT

The SWAT is a conceptual watershed-scale hydrological model designed to address water management, sediment, climate change, land use change, and agricultural chemical yields related challenges (Arnold and Fohrer, 2005; Arnold et al., 2012; Arnold et al., 1998;

Douglas-Mankin et al., 2010; Gassman et al., 2007; Srinivasan et al., 1998b). The SWAT applications range from field scale to watershed scale (Daggupati et al., 2015) to continental scale (Abbaspour et al., 2015; Srinivasan et al., 1998a). The SWAT model components are hydrology, weather, sedimentation, soil temperature, crop growth, nutrients, pesticides, and agricultural management. The hierarchical structure for modeling units in SWAT is set to be multiple sub-watersheds, which are then further subdivided into hydrologic response units (HRUs) that consist of homogeneous land use, management, and soil characteristics. The SWAT simulates the overall hydrologic balance for each HRU and model output is available in daily, monthly, and annual time steps. SWAT meteorological inputs include daily precipitation, maximum and minimum temperature, solar radiation, humidity and wind speed. The version of SWAT used in this work is SWAT2012 rev. 635 (Arnold et al., 2013). The Penman–Monteith method was used to simulate potential evapotranspiration for this work. The SWAT Calibration and Uncertainty Procedures (SWAT-CUP) software package with the Sequential Uncertainty Fitting (SUFI2) method (Abbaspour et al., 2007) was used in model calibration. Watershed stream network and sub-basins were generated using the *Arc SWAT* software (<http://swat.tamu.edu/software/arcswat/>) watershed analysis module (Watershed Delineator) with a contributing area threshold of 253.5km² resulting in 1,138 sub-basins. Applying the HRU module in *Arc SWAT* software with 10% land use percentage over sub-basin area, 10% soil class percentage over land use area, and 10% slope class percentage over soil area, we obtained 10,096 HRUs for the LMRB model.

3. Results

3.1. LMRB Streamflow Statistics

Table 2 gives various statistical measures for the Lower Mekong River annual streamflow using calendar years at different gauges along the main river stem and upstream tributaries. Upper basin inlet streamflow record for the years 2008 and onward, needed for our modeling work, has been regressed from the nearby station (Chiang Sean) streamflow record. The Vientiane (Laos, PDR), station # 011901, the longest monitoring available record compared with other stations studied (1913–2016), has a mean annual streamflow of 4,476 m³/sec. Minimum, maximum, different quantiles, standard deviation, and coefficient of variation values for annual streamflow at different stations are presented. Streamflow stations skewness values suggest the location and the shape of probability distribution (i.e., positive or negative). In Table 2, we also give the Hurst coefficient (Hurst, 1951; Weron, 2002). The Hurst coefficient is an indicator of a serial correlation or dependence for the annual streamflow time series studied. Across the multiple streamflow stations studied at the lower Mekong the Hurst coefficient for annual flows is greater than 0.5 suggesting that high flows most likely will be followed by another high flow in the future. Multiple works have presented various LMRB streamflow statistics (Lacombe et al., 2014; Rossi et al., 2009). However, Table 2 adds a new information - the coefficient of variation, skewness, and persistence and autocorrelation explained by the Hurst coefficient for the Lower Mekong River.

3.2 Calibration and Validation of the LMRB model

SWAT uses many parameters to describe typical soil, plant growth, land cover, reservoir, and agricultural management characteristics. In this work, the LMRB model was calibrated to daily streamflow and monthly average streamflow at the LMRB sub-basin outlets during the 2005 and 2006 with few parameters as outlined in Table 3. Validation of the LMRB model was performed at the LMRB sub-basin outlets during the time period of 2001–2004, and 2007–2015. Parameters used and suggested range values for the LMRB model calibration were consulted and obtained from SWAT developers (*R. Srinivasan, personal communication*) and previous works of *Neitsch et al., (2002)* and *Rossi et al., (2009)*. All other parameters in the LMRB model were left at their default values. Our LMRB model showed higher sensitivity to parameters related to correction factors for precipitation inputs. In general, we found that running our model without remote sensing precipitation data adjustments tend to overestimate simulated streamflow by about 13%. Therefore, we used a separate precipitation correction factor for each sub-basin watershed.

Figure 3 gives observed and simulated daily streamflow at the LMRB (six sub-basins) during the calibration years. The LMRB model is able to explain about 84% of the variance seen in daily streamflow across the Lower Mekong River Basin during the calibration years. In addition, the average percent error (Q_{err}) between daily simulated and observed streamflow across the basin is about 0.86% (Figure 3). We also observe that the Q_{err} and the Nash–Sutcliffe performance metric (NSE) in calibration of our model at monthly results varies between -1.9% and 4.76% and 0.91 and 0.96 for the six sub-basins, respectively (Figure 4). The calibrated value for the soil evaporation compensation factor parameter ($ESCO = 0.6$) is found to be lower than previous values reported by *Rossi et al., (2009)* for the LMRB. Generally, as the value for $ESCO$ is reduced the SWAT model is able to extract more of the evaporative demand from lower soil layers. We argue here that the newer soil data used in this work has influenced a newer value of $ESCO$ for the LMRB different than the default one previously used (i.e., $ESCO = 0.95$). The parameters listed in Table 3 are among many parameters that describe the SWAT soil physical characteristics and influence the movement of water and air through the soil profile and shallow aquifer underneath it, thus they have a major impact on the cycling of water within the SWAT modeling unit (HRU).

Figure 5 gives monthly observed and simulated streamflow for the study watershed in validation of the LMRB model during 13 years. In general, the model captured the timing of onset and end of seasonal streamflow but was slightly off in some estimates of peak flows. The NSE metric during validation time period for our model varies between 0.86 and 0.95 . The model has about 3.85% error on average in estimating monthly flows during the validation time period. Our LMRB model evaluation results are similar to previous attempts presented by *Rossi et al., (2009)* who reported a Nash-Sutcliffe flow monthly efficiency values ranging between 0.8 and 1.0 at mainstream monitoring stations.

3.3 LMRB Flow Regime

In this study, the experiment we performed covered the LMRB model scenario analyses. Hypothetical scenarios of reducing and increasing the UMRB flow inputs during June, July,

August, and September months by up to 30% of the existing flows conditions have been examined and tracked downstream. Lower Mekong flow records at these specific months (June, July, August, and September) are usually very high compared with other flow records during the year (Figure 6). Figure 6 gives the streamflow daily variation at Vientiane (Sub-basin 3) during 1913 to 2016.

The Mekong River historical streamflow data suggests that the river has a high streamflow variability. The *DAYCV* at Sub-basin 7 and Sub-basin 8 river sections varies between 117% to 154%. Results showed that the downstream river section Sub-basin 6 has a higher *DAYCV* compared with upstream river section Sub-basin 1 (Table 4). We attribute this phenomenon to the fact that the Mekong River is a highly regulated river system with many reservoirs that have different operation plans. This complexity in managing the river sections has resulted in a trend of *DAYCV* increase as we move downstream the Mekong River. Upon examination of the streamflow variability (*DAYCV*) with changes in upstream releases to the Lower Mekong, we found that flow variability is pronounced at SB1 and decreases as we go downstream till SB6. Sub-basin 1 *DAYCV* varies between 20% to -2%, while Sub-basin 6 *DAYCV* varies between 1-2% (Table 4). We infer here that the streamflow coefficient of variation changes would be clearly seen at the upper part of the Lower Mekong specially when more flows are released from the upstream Mekong River.

Analysis of the Lower Mekong River historical streamflow data during 2001-2015 using the Colwell index metrics indicates that the flow has a low predictability (average of $P \approx 32\%$). The Constancy (*C*) at the observed historical predictability is on average of 26%. This suggests that the Mekong River streamflow gauges predictability are due to high constancy of streamflow which varies little among months and years studied (Figure 7 and Figure 8). Therefore, the streamflow discharge at the Lower Mekong (which never varies across seasons during years studied) is perfectly predictable with all the predictability deriving from the constancy component.

Upon changing the inflow input from upstream, the downstream streamflow predictability has been reduced further. In Figure 7, we give at three sub-basins (SB4, SB5, and SB6) the percent change in predictability (*P*) as a result of upstream input flow changes. We realize that any change in input flow, whether it is increase or decrease in input flow, reduces the predictability at the LMRB. However, upstream input flow increases affect the Colwell predictability more than upstream input flow decreases. This corroborates with the expected flooding in LMRB as a result of upstream higher input flows. For example, in Figure 7, SB4 sensitivity results (top panel) suggests that increasing the upstream flow by 30% more than existing current conditions would result in reducing the predictability (*P*) by about 33% to be 0.23 (current *P* at SB4 is equal to 0.34).

Looking at Kratie, Cambodia (SB6) in Figure 8, we see that releasing more water from upstream Mekong during raining months by 30% would mean a reduction in predictability by 21%. This reduction in predictability is mainly attributed to a reduction in the Contingency index. Since Contingency represents the degree to which time determines state, or the degree to which they are dependent on each other. This can be translated to a change in flooding occurrence times. This streamflow predictability findings can be generalized at

the whole Lower Mekong by saying that our ability to predict floods/droughts in general would be reduced if there is any change (i.e., increase/decrease) anticipated from upstream Mekong releases.

The other streamflow variability pattern we studied in this work was flow reversals (*FLOWREV*). We found that flow reversals are showing a notable increasing trend across the LMRB (Figure 9). We think that this observation of striking increase in flow reversal days is mainly due to the effect of flow regulations in the Mekong River Basin (Upper and Lower). Upon examining flow reversals trends when input releases from upstream Mekong are changed, we found that in general flow reversal days are increasing. This means a higher flow variability would be experienced upon changing input releases.

Our analysis of high flow disturbance for the Lower Mekong River streamflow regime covered seven-day maximum flow and flood duration variables. Mann Kendall trend analysis for seven-day maximum flow (*7QMAX*) was used to examine whether any trends in maximum flows were statistically significant. Table 5 gives Mann Kendall trend analysis results for the historic seven-day maximum flow as well as seven-day maximum flow when input flow releases from upstream Mekong were adjusted. In general, we found that there is decreasing trend of *7QMAX* across the whole lower Mekong during time period studied (e.g., 2001–2015) with an average *7QMAX* value varies from 3 to 6 millimeters per day at Sub-basin 1 and Sub-basin 6. We correlate the observed decreasing trend of *7QMAX* and the increasing trend of *7QMIN* (results not shown) to the increased number of flow reversals seen earlier in Figure 9. That means increased number of flow reversals are increased number of days with low flow changes.

Another high flow disturbance variable studied in this work was flood duration (*FLDDUR*). Generally, flood durations within the LMRB are long and more frequent specially at Mukdahan, Thailand and southward (Figure 10). For instance, on 2011 the streamflow gauge discharge record at Mukdahan recorded 13 days with discharges equal to or exceed a threshold of 30,400 m³/sec (equivalent to 12.6 meters as a stage height). Our results reveal that releasing more flows from the UMRB (i.e., 30% increase) at the same year of 2011, would have caused the same streamflow gauge to record 16 days of discharges equal to or exceed the flood threshold. Our results also show that releasing more flows from the UMRB would also affect the frequency of flood occurrences. Therefore, changing flow releases from upstream Mekong need to be carefully examined since not only flood duration is going to change but also flood occurrences is going to change too.

4. Discussion

SWAT is the choice of watershed model by many stakeholders in the Mekong Basin region for their decision framework, including the Mekong River Commission, and has been identified in the SERVIR-Mekong Regional Needs Assessment (NASA, 2014). We have used multiple satellite-based earth observation systems and a spatial data to build up a hydrologic model (SWAT) for the Lower Mekong River Basin. Our objective to develop a physically based hydrological model at the LMRB was to better understand the impacts associated with UMRB water changes on the LMRB streamflow variability, and flood

frequency and duration. Multiple streamflow regime variables were examined across the Lower Mekong under different scenarios of UMRB water releases. Our modeling efforts presented are thought to be in line with a substantial body of literature that discusses the Lower Mekong River hydrological change under expected and on-going hydropower development and climate change effects (Li et al., 2017; Lyon et al., 2017; Piman et al., 2016; Piman et al., 2013b). Growing populations, and the staggering effects of climate change that are seen in high temperatures, and variable precipitation patterns over the Mekong River raise the potential for shifts in the hydrological responses at the Lower Mekong Basin. Having updated statistics on streamflow information at the LMRB is then needed given the ongoing regional development occurring at the basin in terms of agricultural expansion and infrastructure development.

The Lower Mekong flow variability and predictability conditions will be directly affected in terms of increased flow variability and decreased flow predictability due to changing input flow releases from the UMRB. Releasing more water from the UMRB during rainy season (for instance by 30%) would imply a further reduction in the Lower Mekong streamflow predictability (i.e., Colwell index reduces to 25%). Stream ecologists such as *Resh et al.*, (1988) and *Lazzaro et al.*, (2013) are often interested in studying streamflow regime because of its relation to channel disturbance. Our work suggested that flow releases increase from the UMRB would mean more flooded days as well as higher frequency of flood occurrences specially at Mukdahhan (Thailand), Pakse (Laos), and Kratie (Cambodia). This is an alarming finding since the fate of many people and properties will be at stake.

Models results are often uncertain. The model simulation efficiencies have to be considered in examining the results of this work. The uncertainty and limitations seen are due to the nature of modelling that could be related to error in model data inputs, parameters and process representation. It is worth to mention here that the LMRB models' performance comparison was based on monthly flows output, so some amount of temporal and spatial aggregation may have masked individual event prediction or adds uncertainty. We do agree that model results such as the ones presented in this work should be thought and considered as tools used to efficiently and collaboratively guide decision makers. In conclusion, collaborative work and sharing information between the upstream and downstream Mekong River agencies and stakeholders is critically needed to successfully manage the precious Mekong River. Remote sensing data can aide and has achieved a nice job in addressing hydrologic modeling needs and requirements at the Lower Mekong River Basin.

Supplementary Material

Refer to Web version on PubMed Central for supplementary material.

Acknowledgements

This work was fully supported by the National Aeronautics and Space Administration (NASA), Goddard Space Flight Center (GSFC) Applied Sciences Grants NNX16AT88G, NNX16AT86G, and NNG15HQ01C. Special thanks are extended to Joe Spruce who processed and shared with us the Land Use/Land Cover map for the Lower Mekong Basin. Any opinions, findings, and conclusions or recommendations expressed in this work are those of the author(s) and do not necessarily reflect the views of the National Aeronautics and Space Agency, Science Systems and Applications, Inc., and Science Applications International Corporation.

Appendix A

6.

6. A.1.: Dams Data

Data for existing dams within the Mekong Basin was obtained from the Greater Mekong Consultative Group for International Agricultural Research (CGIAR) Program on Water, Land and Ecosystems (WLE, 2017). In Figure 1, we depict dams within the Lower Mekong River Basin that are either already commissioned or still under construction and have a maximum reservoir area greater than or equal to 280 km² similar to the MRC SWAT model setup. The surface area of the reservoirs behind the various dams that we have included in this study are listed in Table A. 1.

6. A.2.: nasaaccess

The ‘nasaaccess’ package with R software (R Development Core Team, 2017) current version (*nasaaccess* version 1.2) processes remote sensing data products (i.e., TRMM, GPM, and GLDAS) and creates weather input definition tables as well as stations data files in a format readable by SWAT model or any other rainfall/runoff model. The *nasaaccess* package can be expanded to include other remote sensing products needed in future. For the time being, *nasaaccess* generates daily rainfall and minimum and maximum air temperatures gridded data and gridded data definition files needed to serve as a setup for any basic SWAT/other model run. The core functionality of the *nasaaccess* package access NASA Goddard Space Flight Center (GSFC) servers to download climate data, clip needed grids based on a user study watershed, handles temporal issues (e.g., GLDAS product has 3-hour temporal resolution), and then generates daily climate gridded data files and definition files compatible with SWAT/other models. The inputs needed for the various functions within the *nasaaccess* are: start and end dates for a user climate data simulation period, and a shapefile and a DEM grid for a study watershed.

6. A.3.: streamflow regime metrics

The coefficient of variation variable (*DAYCV*) is defined as the standard deviation of daily flows divided by the average of daily flows multiplied by 100 during a year. The annual coefficient of variation can be expressed as:

$$DAYCV = \frac{\sigma}{\mu} \times 100 \quad , \quad (A.3.1)$$

where (M) is the unbiased standard deviation (denominator is $n - 1$), and μ is the arithmetic mean during a year of flow records. The *DAYCV* describes overall the flow variability regardless of sequential flow variations. Generally, flow variability is lower in downstream than upstream river sections (Horwitz, 1978).

Flow reversals (*FLOWREV*) are defined here from the daily streamflow as days when the trend (increasing or decreasing) from the previous days is reversed. Flow reversals are calculated by counting the days when flow records are higher (rising) or lower (falling) than previous day records. This can be explained as:

FLOWREV is counted when

$$\begin{cases} \text{sign}(DQ_j) \text{ is positive \& sign}(DQ_{j-1}) \text{ is zero or negative} \\ \text{sign}(DQ_j) \text{ is negative \& sign}(DQ_{j-1}) \text{ is zero or positive} \end{cases} \quad (\text{A.3.2})$$

where $DQ = \text{diff}(Q)$, $\text{diff}(Q)$ is flow lagged differences, and Q is a daily flow vector, and $\text{sign}(DQ_j)$ is the sign of the corresponding element in lagged difference vector DQ .

Colwell's indices (Colwell, 1974) are flow predictability metrics developed to assess relevant measures of flow variability (e.g., biological). The principal value of the Colwell index used in our work is for comparison of the uncertainty of the variable river environment projected due to upper stream changes. The Colwell procedure is analogous to autocorrelation analysis and to some aspects of harmonic analysis. The Colwell's predictability (P) is the sum of constancy (C) and contingency (M). Constancy (C) is a measure of temporal invariance, and contingency (M) is a measure of periodicity. Constancy is defined similar to predictability, except that seasonal variability across periods is disregarded. Contingency is defined as the degree to which time period and value group are dependent on each other. The P , C , and M are scaled to range from 0 to 1. Further details on Colwell index are presented at Appendix B in *Mohammed et al. (2015)*.

Calculation of Colwell's indices requires that streamflow values be binned into discrete groups. As with all information measures absolute values are dependent on this binning, but a consistent binning allows relative comparisons. Following *Mohammed et al. (2015)* and others, we used 7 bins ($< 0.5\mu, 1.0\mu, 1.5\mu, 2.0\mu, 2.5\mu, 3.0\mu, > 3.0\mu$), where μ is equal to the mean of daily streamflow values, to define groups for dry and flood seasons of the streamflow record. These two seasons represent the seasonal cycle for the LMRB and we counted the number of occurrences of daily streamflow values in states defined by groups (bins) and periods (seasons) to arrive at the Colwell's indices. Dry season time period is from January 1st to May 31st and flood season time period is from June 1st to December 31st. Following Colwell, for a frequency matrix (contingency table) with t columns (times within a cycle) and s rows (state of the phenomenon). Let N_{ij} be the number of cycles for which the phenomenon was in state i at time j . Define the column totals (X_j), row totals (Y_i), and the grand total (Z) as:

$$X_j = \sum_{i=1}^s N_{ij}, \quad Y_i = \sum_{j=1}^t N_{ij}, \quad \text{and} \quad Z = \sum_i \sum_j N_{ij} = \sum_j X_j = \sum_i Y_i$$

(A.3.3)

Then, the uncertainty with respect to time is:

$$H(X) = - \sum_{j=1}^t \frac{X_j}{Z} \log \frac{X_j}{Z} \quad (\text{A.3.4})$$

the uncertainty with respect to state is:

$$H(Y) = - \sum_{i=1}^s \frac{Y_i}{Z} \log \frac{Y_i}{Z} \quad (\text{A.3.5})$$

and the uncertainty with respect to the interaction of time and state is:

$$H(XY) = - \sum_i \sum_j \frac{N_{ij}}{Z} \log \frac{N_{ij}}{Z} \quad (\text{A.3.6})$$

The predictability of a periodic phenomenon is maximal when there is complete certainty with regard to state (row) once the point in time (column) is specified. In terms of information theory, the conditional uncertainty with regard to state, with time given, is defined as: $H_X(Y) = H(XY) - H(X)$ (Jelínek, 1968). When predictability is at its minimum, all states are equiprobable for all times. In this case $H(X) = \log t$, and $H(XY) = \log st$, so that $H_X(Y) = \log s$. To obtain measure of predictability (P) with the range (0, 1), define:

$$P = 1 - \frac{H_X(Y)}{\log s} = 1 - \frac{H(XY) - H(X)}{\log s} \quad (\text{A.3.7})$$

Constancy is maximized when all row totals equal to zero with the exception of a single row total being greater than zero; it is minimized when all row totals are equal. Since $H(Y)$ varies in precisely the opposite way, and its maximum value is $\log s$, a measure of constancy (C) with range (0, 1) is given by:

$$C = 1 - \frac{H(XY)}{\log s} \quad (\text{A.3.8})$$

Contingency represents the degree to which time determines state, or the degree to which they are dependent on each other. In information theory, contingency is measured by a quantity called average mutual information (Jelínek, 1968). *Colwell* (1974) cites contingency as the average amount of information about the state of the phenomenon provided by time or $I(XY) = H(Y) - H_X(Y) = H(Y) + H(X) - H(XY)$. *Colwell* (1974) gives an adjusted measure of contingency (M), with range (0, 1) as:

$$M = \frac{H(X) + H(Y) - H(XY)}{\log s} \quad (\text{A.3.9})$$

Flood duration (*FLDDUR*) is usually calculated as the average number of days per year when flow equals or exceeds flood threshold flow. Since the LMRB is a complex system, estimating the magnitude of daily return flow that we can use in calculating flood duration periods is quite challenging. Upon compilation of several MRC weekly flood situation reports (<http://ffw.mrcmekong.org/>), we extracted the flood stage height threshold and then estimated the daily return flow using the stage-flow relation along the LMRB. The flood stage heights along the LMRB are: 11.8 meters at Chiang Sean (station # 010501), 18 meters at Luang Prabang (station # 011201), 12.6 meters at Vientiane (station #011901), 12.6 meters Mukdahan (station # 013402), 12.0 meters at Pakse (station # 013901), and 23.0 meters at Kratie (station # 014901). These stage heights correspond to the following flows 18,535; 17,950; 22,399; 30,400; 38,930; 58,256 m³/sec respectively. We used these flood thresholds at each sub-basin outlet to calculate flood duration periods for this work.

Seven-day maximum flow (*7QMAX*) is the average across years of 7-day maximum streamflow. For each year in the period of record, the maximum 7-day mean is found from the daily mean streamflow and the maximum is the 7-day maximum flow for that year.

7. References

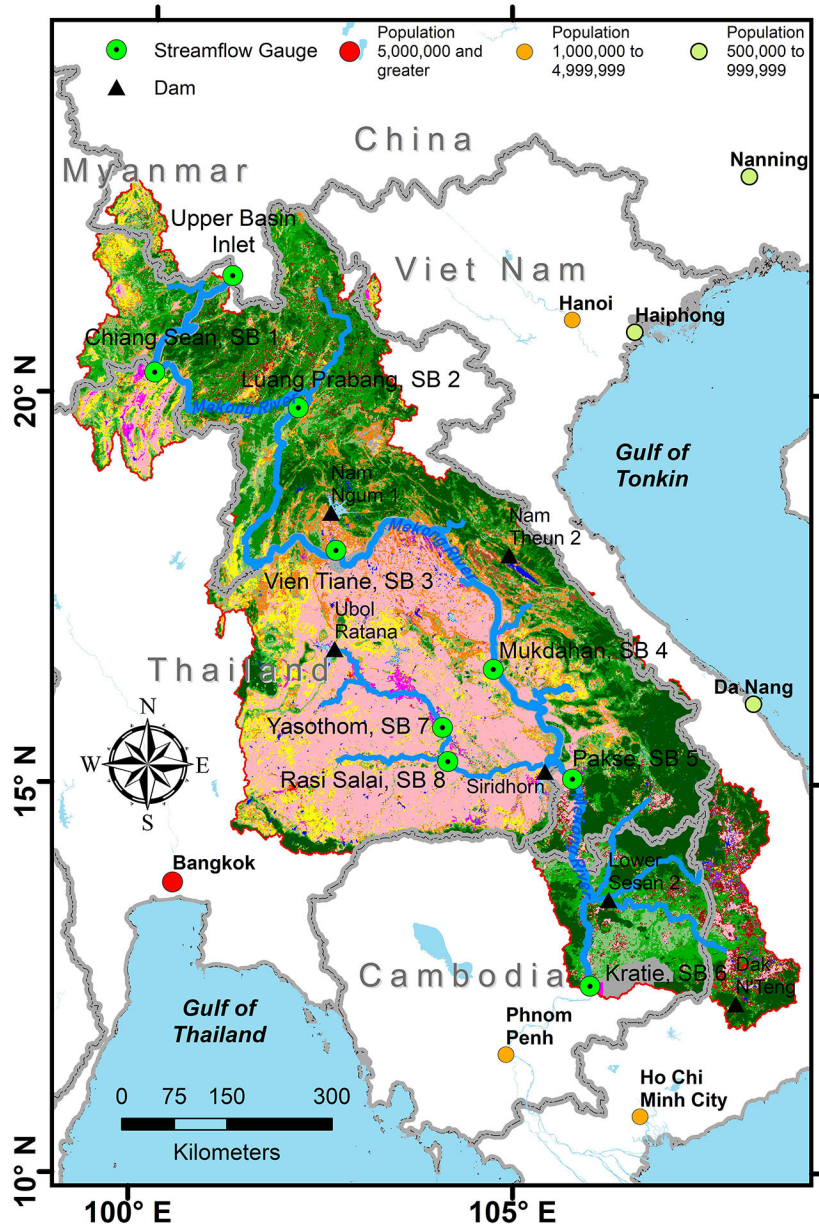
- Abbaspour KC , Rouholahnejad E , Vaghefi S , Srinivasan R , Yang H , Kløve B , 2015 A continental-scale hydrology and water quality model for Europe: Calibration and uncertainty of a high-resolution large-scale SWAT model. *J. Hydrol* 524, 733–752, 10.1016/j.jhydrol.2015.03.027
- Abbaspour KC , Yang J , Maximov I , Siber R , Bogner K , Mieleitner J , Zobrist J , Srinivasan R , 2007 Modelling hydrology and water quality in the pre-alpine/alpine Thur watershed using SWAT. *J. Hydrol* 333, 413–430, 10.1016/j.jhydrol.2006.09.014
- Arnold JG , Fohrer N , 2005 SWAT2000: Current capabilities and research opportunities in applied watershed modelling. *Hydrol. Process* 19, 563–572, 10.1002/hyp.5611
- Arnold JG , Kiniry JR , Srinivasan R , Williams JR , Haney EB , Neitsch SL , 2013 SWAT 2012 Input/Output documentation TR-439, Texas Water Resources Institute, College Station, TX.
- Arnold JG , Moriasi DN , Gassman PW , Abbaspour KC , White MJ , Srinivasan R , Santhi C , Harmel RD , Griensven A.v. , Liew MWV , Kannan N , Jha MK , 2012 SWAT: Model use, calibration, and validation. *T ASABE* 55, 1491–1508, 10.13031/2013.42256

- Arnold JG , Srinivasan R , Muttiah RS , Williams JR , 1998 Large area hydrologic modeling and assessment part I: Model development. *J. Am. Water Resour. As* 34, 73–89, 10.1111/j.1752-1688.1998.tb05961.x
- Ceola S , Montanari A , Koutsoyiannis D , 2014 Toward a theoretical framework for integrated modeling of hydrological change. *Wiley Interdisciplinary Reviews: Water* 1, 427–438, 10.1002/wat2.1038
- Cochrane TA , Arias ME , Piman T , 2014 Historical impact of water infrastructure on water levels of the Mekong River and the Tonle Sap system. *Hydrol. Earth Syst. Sci* 18, 4529–4541, 10.5194/hess-18-4529-2014
- Colwell RK , 1974 Predictability, constancy, and contingency of periodic phenomena. *Ecology* 55, 1148–1153, 10.2307/1940366
- Daggupati P , Yen H , White MJ , Srinivasan R , Arnold JG , Keitzer CS , Sowa SP , 2015 Impact of model development, calibration and validation decisions on hydrological simulations in West Lake Erie Basin. *Hydrol. Process* 29, 5307–5320, 10.1002/hyp.10536
- DeFries R , Eshleman KN , 2004 Land-use change and hydrologic processes: A major focus for the future. *Hydrol. Process* 18, 2183–2186, 10.1002/hyp.5584
- Delgado JM , Apel H , Merz B , 2010 Flood trends and variability in the Mekong River. *Hydrol. Earth Syst. Sci* 14, 407–418, 10.5194/hess-14-407-2010
- Douglas-Mankin KR , Srinivasan R , Arnold JG , 2010 Soil and Water Assessment Tool (SWAT) model: Current developments and applications. *T ASABE* 53, 1423–1431, 10.13031/2013.34915
- Dudgeon D , Arthington AH , Gessner MO , Kawabata Z-I , Knowler DJ , L ev eque C , Naiman RJ , Prieur-Richard A-H , Soto D , Stiassny MLJ , Sullivan CA , 2006 Freshwater biodiversity: importance, threats, status and conservation challenges. *Biol. Rev* 81, 163–182, 10.1017/S1464793105006950 [PubMed: 16336747]
- FAO, IIASA, ISRIC-World Soil Information, Institute of Soil Science, Chinese Academy of Sciences (ISSCAS), Joint Research Centre of the European Commission (JRC), Harmonized World Soil Database, v1.21, 2012 <http://www.fao.org/soils-portal/soil-survey/soil-maps-and-databases/harmonized-world-soil-database-v12/en/>
- Gassman PW , Reyes MR , Green CH , Arnold JG , 2007 The soil and water assessment tool: Historical development, applications, and future research directions. *T ASABE* 50, 1211–1250, 10.13031/2013.23637
- Gleick PH , 2000 A Look at twenty-first century water resources development. *Water Int* 25, 127–138, 10.1080/02508060008686804
- Grafton RQ , Pittock J , Davis R , Williams J , Fu G , Warburton M , Udall B , McKenzie R , Yu X , Che N , Connell D , Jiang Q , Kompas T , Lynch A , Norris R , Possingham H , Quiggin J , 2013 Global insights into water resources, climate change and governance. *Nat. Clim. Change* 3, 315–321, 10.1038/nclimate1746
- Haddeland I , Lettenmaier DP , Skaugen T , 2006 Effects of irrigation on the water and energy balances of the Colorado and Mekong river basins. *J. Hydrol* 324, 210–223, 10.1016/j.jhydrol.2005.09.028
- He Z , Yang L , Tian F , Ni G , Hou A , Lu H , 2017 Intercomparisons of rainfall estimates from TRMM and GPM multisatellite products over the Upper Mekong River Basin. *J. Hydrometeorol* 18, 413–430, 10.1175/jhm-d-16-0198.1
- Heistermann M , 2017 HESS opinions: A planetary boundary on freshwater use is misleading. *Hydrol. Earth Syst. Sci* 21, 3455–3461, 10.5194/hess-21-3455-2017
- Helsel DR , Hirsch RM , 2002 *Statistical Methods in Water Resources, Techniques of Water-Resources Investigations of the United States Geological Survey Book 4, Hydrologic Analysis and Interpretation*. U.S. Geol. Sur, Reston, VA, pp. 522.
- Hester ET , Doyle MW , 2011 Human impacts to river temperature and their effects on biological processes: A quantitative synthesis. *J. Am. Water Resour. As* 47, 571–587, 10.1111/j.1752-1688.2011.00525.x
- Hoang LP , Lauri H , Kumm M , Koponen J , van Vliet MTH , Supit I , Leemans R , Kabat P , Ludwig F , 2016 Mekong River flow and hydrological extremes under climate change. *Hydrol. Earth Syst. Sci* 20, 3027–3041, 10.5194/hess-20-3027-2016

- Horwitz RJ , 1978 Temporal variability patterns and the distributional patterns of stream fishes. *Ecol. Monogr* 48, 307–321, 10.2307/2937233
- Hurst HE , 1951 Long-term storage capacity of reservoirs. *T. Am. Soc. Civ. Eng* 116, 770–808
- Jacobs JW , 2002 The Mekong River Commission: Transboundary water resources planning and regional security. *Geogr. J* 168, 354–364, 10.1111/j.0016-7398.2002.00061.x [PubMed: 17494227]
- Jelínek F , 1968 Probabilistic Information Theory: Discrete and Memoryless Models. McGraw-Hill, New York, 609 pp.
- Kite G , 2001 Modelling the Mekong: Hydrological simulation for environmental impact studies. *J. Hydrol* 253, 1–13, 10.1016/S0022-1694(01)00396-1
- Kottegoda NT , Rosso R , 1997 Probability, Statistics, and Reliability for Civil and Environmental Engineers. McGraw-Hill, New York, 735 pp.
- Kummu M , Sarkkula J , 2008 Impact of the Mekong River flow alteration on the Tonle Sap flood pulse. *AMBIO* 37, 185–192, 10.1579/0044-7447(2008)37[185:IOTMRF]2.0.CO;2 [PubMed: 18595273]
- Lacombe G , Douangsavanh S , Vogel RM , McCartney M , Chemin Y , Rebelo L-M , Sotoukee T , 2014 Multivariate power-law models for streamflow prediction in the Mekong Basin. *J. Hydrol. Reg. St* 2, 35–48, 10.1016/j.ejrh.2014.08.002
- Lakshmi V , 2004 The role of satellite remote sensing in the prediction of ungauged basins. *Hydrol. Process* 18, 1029–1034, 10.1002/hyp.5520
- Lazzaro G , Basso S , Schirmer M , Botter G , 2013 Water management strategies for run-of-river power plants: Profitability and hydrologic impact between the intake and the outflow. *Water Resour. Res* 49, 8285–8298, 10.1002/2013wr014210
- Li D , Long D , Zhao J , Lu H , Hong Y , 2017 Observed changes in flow regimes in the Mekong River Basin. *J. Hydrol* 551, 217–232, 10.1016/j.jhydrol.2017.05.061
- Lu Xi Xi WJ-J , Grundy-Warr C , 2008 Are the Chinese dams to be blamed for the lower water levels in the Lower Mekong? In: Kummu M , Keskinen M , Varis O (Eds.), *Modern Myths of the Mekong : A critical review of water and development concepts, principles and policies*. Water and development publications, 01. Helsinki University of Technology, Espoo, Finland, pp. 39–51.
- Lyon SW , King K , Polpanich O. u. , Lacombe G , 2017 Assessing hydrologic changes across the Lower Mekong Basin. *J. Hydrol. Reg. St* 12, 303–314, 10.1016/j.ejrh.2017.06.007
- Mainuddin M , Kirby M , 2009 Agricultural productivity in the Lower Mekong Basin: Trends and future prospects for food security. *Food Secur.* 1, 71–82, 10.1007/s12571-008-0004-9
- Mekong River Commission, 2009a The Flow of the Mekong. No. 2, Mekong River Commission Secretariat, Vientiane, Lao PDR.
- Mekong River Commission, 2009b MRC's Role in Agriculture and Agricultural Water Management, Mekong River Commission Secretariat, Vientiane, Lao PDR.
- Mekong River Commission, 2017 Transboundary water resources management issues in the Mekong Delta of Cambodia and Viet Nam, Mekong River Commission Secretariat, Vientiane, Lao PDR.
- Milly PCD , Betancourt J , Falkenmark M , Hirsch RM , Kundzewicz ZW , Lettenmaier DP , Stouffer RJ , 2008 Stationarity is dead: Whither water management? *Science* 319, 573–574, 10.1126/science.1151915 [PubMed: 18239110]
- Milly PCD , Dunne KA , Vecchia AV , 2005 Global pattern of trends in streamflow and water availability in a changing climate. *Nature* 438, 347–350, 10.1038/nature04312 [PubMed: 16292308]
- Mohammed IN , Bomblies A , Wemple BC , 2015 The use of CMIP5 data to simulate climate change impacts on flow regime within the Lake Champlain Basin. *J. Hydrol. Reg. St* 3, 160–186, 10.1016/j.ejrh.2015.01.002
- Montanari A , Young G , Savenije HHG , Hughes D , Wagener T , Ren LL , Koutsoyiannis D , Cudennec C , Toth E , Grimaldi S , Blöschl G , Sivapalan M , Beven K , Gupta H , Hipsey M , Schaeffli B , Arheimer B , Boegh E , Schymanski SJ , Di Baldassarre G , Yu B , Hubert P , Huang Y , Schumann A , Post DA , Srinivasan V , Harman C , Thompson S , Rogger M , Viglione A , McMillan H , Characklis G , Pang Z , Belyaev V , 2013 “Panta Rhei—Everything Flows”: Change

- in hydrology and society—The IAHS Scientific Decade 2013–2022. *Hydrolog. Sci. J* 58, 1256–1275, 10.1080/02626667.2013.809088
- Mosley LM , 2015 Drought impacts on the water quality of freshwater systems; Review and integration. *Earth-Sci. Rev* 140, 203–214, 10.1016/j.earscirev.2014.11.010
- NASA, 2014 SERVIR Annual Report, United States Agency for International Development and the National Aeronautics and Space Administration, Huntsville, AL.
- Neitsch SL , Arnold JG , Kiniry JR , Williams JR , King KW , 2002 Soil and Water Assessment Tool theoretical documentation version 2000 TR-191, Texas Water Resources Institute, College Station, TX.
- Piman T , Cochrane TA , Arias ME , 2016 Effect of Proposed Large Dams on Water Flows and Hydropower Production in the Sekong, Sesan and Srepok Rivers of the Mekong Basin. *River Res. Appl* 32, 2095–2108, 10.1002/rra.3045
- Piman T , Cochrane TA , Arias ME , Green A , Dat ND , 2013a Assessment of flow changes from hydropower development and operations in Sekong, Sesan, and Srepok Rivers of the Mekong Basin. *J. Water Res. Plan. Man* 139, 723–732, 10.1061/(ASCE)WR.1943-5452.0000286
- Piman T , Lennaerts T , Southalack P , 2013b Assessment of hydrological changes in the Lower Mekong Basin from Basin-Wide development scenarios. *Hydrol. Process* 27, 2115–2125, 10.1002/hyp.9764
- Poff N , 1996 A hydrogeography of unregulated streams in the United States and an examination of scale-dependence in some hydrological descriptors. *Freshwater Biol.* 36, 71–79, 10.1046/j.1365-2427.1996.00073.x
- Poff NL , Allan JD , Bain MB , Karr JR , Prestegard KL , Richter BD , Sparks RE , Stromberg JC , 1997 The natural flow regime. *BioScience* 47, 769–784, 10.2307/1313099
- Poff NL , Olden JD , 2017 Can dams be designed for sustainability? *Science* 358, 1252–1253, 10.1126/science.aaq1422 [PubMed: 29217554]
- R Development Core Team, 2017 R: A language and environment for statistical computing R Found. for Stat. Comput, Vienna, Austria.
- Räsänen TA , Koponen J , Lauri H , Kumm M , 2012 Downstream hydrological impacts of hydropower development in the Upper Mekong Basin. *Water Resour. Manag* 26, 3495–3513, 10.1007/s11269-012-0087-0
- Räsänen TA , Someth P , Lauri H , Koponen J , Sarkkula J , Kumm M , 2017 Observed river discharge changes due to hydropower operations in the Upper Mekong Basin. *J. Hydrol* 545, 28–41, 10.1016/j.jhydrol.2016.12.023
- Resh VH , Brown AV , Covich AP , Gurtz ME , Li HW , Minshall GW , Reice SR , Sheldon AL , Wallace JB , Wissmar RC , 1988 The role of disturbance in stream ecology. *J. N. Am. Benthol. Soc* 7, 433–455, 10.2307/1467300
- Rodell M , Houser PR , Jambor U , Gottschalck J , Mitchell K , Meng C-J , Arsenault K , Cosgrove B , Radakovich J , Bosilovich M , Entin JK , Walker JP , Lohmann D , Toll D , 2004 The global land data assimilation system. *B. Am. Meteorol. Soc* 85, 381–394, 10.1175/bams-85-3-381
- Rossi CG , Srinivasan R , Jirayoot K , Duc TL , Souvannabouth P , Binh N , Gassman PW , 2009 Hydrologic evaluation of the Lower Mekong River Basin with the soil and water assessment tool model. *IAEJ* 18, 1–13, <http://114.255.9.31/iaej/EN/Y2009/V18/I01-02/1>
- Sabo JL , Ruhi A , Holtgrieve GW , Elliott V , Arias ME , Ngor PB , Räsänen TA , Nam S , 2017 Designing river flows to improve food security futures in the Lower Mekong Basin. *Science* 358, 10.1126/science.aao1053
- Spruce J , Bolten JD , Srinivasan R , 2017 Developing land use land cover maps for the Lower Mekong Basin to aid SWAT hydrologic modeling, in: 2017 AGU Fall Meeting, Abstract H104–298677. AGU, New Orleans, Louisiana.
- Srinivasan R , Arnold JG , Jones CA , 1998a Hydrologic modelling of the United States with the soil and water assessment tool. *Int. J. Water Resour. D* 14, 315–325, 10.1080/07900629849231
- Srinivasan R , Ramnarayanan TS , Arnold JG , Bednarz ST , 1998b Large area hydrologic modeling and assessment part II: Model application. *J. Am. Water Resour. As* 34, 91–101, 10.1111/j.1752-1688.1998.tb05962.x

- Thanh DD , Cochrane TA , Arias ME , Tri VPD , Vries TD , 2015 Analysis of water level changes in the Mekong floodplain impacted by flood prevention systems and upstream dams, in: The 36th IAHR World Congress. Hague, Netherlands.
- Veilleux JC , Anderson EP , 2016 2015 Snapshot of water security in the Nile, Mekong, and Amazon River Basins. *Limnol. Oceanogr.-Bull* 25, 8–14, 10.1002/lob.10085
- Vörösmarty CJ , McIntyre PB , Gessner MO , Dudgeon D , Prusevich A , Green P , Glidden S , Bunn SE , Sullivan CA , Liermann CR , Davies PM , 2010 Global threats to human water security and river biodiversity. *Nature* 467, 555–561, 10.1038/nature09440 [PubMed: 20882010]
- Wang C , 2017 Study on the adverse effects of hydropower development on international shipping. *IOP Conf. Ser.: Earth Environ. Sci* 61, 012063, 10.1088/1755-1315/61/1/012063
- Wang W , Lu H , Ruby Leung L , Li HY , Zhao J , Tian F , Yang K , Sothea K , 2017a Dam construction in Lancang-Mekong River Basin could mitigate future flood risk from warming-induced intensified rainfall. *Geophys. Res. Lett* 44, 10378–10386, 10.1002/2017GL075037
- Wang W , Lu H , Yang D , Sothea K , Jiao Y , Gao B , Peng X , Pang Z , 2016 Modelling Hydrologic Processes in the Mekong River Basin Using a Distributed Model Driven by Satellite Precipitation and Rain Gauge Observations. *PLOS ONE* 11, e0152229, 10.1371/journal.pone.0152229 [PubMed: 27010692]
- Wang W , Lu H , Zhao T , Jiang L , Shi J , 2017b Evaluation and comparison of daily rainfall from latest GPM and TRMM products over the Mekong River Basin. *IEEE J. Sel. Top. Appl* 10, 2540–2549, 10.1109/JSTARS.2017.2672786
- Weron R , 2002 Estimating long-range dependence: Finite sample properties and confidence intervals. *Physica A* 312, 285–299, 10.1016/S0378-4371(02)00961-5
- Wild TB , Loucks DP , 2014 Managing flow, sediment, and hydropower regimes in the Sre Pok, Se San, and Se Kong Rivers of the Mekong basin. *Water Resour. Res* 50, 5141–5157, 10.1002/2014WR015457
- Winemiller KO , McIntyre PB , Castello L , Fluet-Chouinard E , Giarrizzo T , Nam S , Baird IG , Darwall W , Lujan NK , Harrison I , Stiassny MLJ , Silvano RAM , Fitzgerald DB , Pelicice FM , Agostinho AA , Gomes LC , Albert JS , Baran E , Petrere M , Zarfl C , Mulligan M , Sullivan JP , Arantes CC , Sousa LM , Koning AA , Hoenighaus DJ , Sabaj M , Lundberg JG , Armbruster J , Thieme ML , Petry P , Zuanon J , Vilara GT , Snoeks J , Ou C , Rainboth W , Pavanelli CS , Akama A , Soesbergen A.v. , Sáenz L , 2016 Balancing hydropower and biodiversity in the Amazon, Congo, and Mekong. *Science* 351, 128–129, 10.1126/science.aac7082 [PubMed: 26744397]
- WLE, Dataset on the dams of the Irrawaddy, Mekong, Red and Salween River Basins, 2017 <https://wle-mekong.cgiar.org/maps/>
- Zhang B , Zhang L , Guo H , Leinenkugel P , Zhou Y , Li L , Shen Q , 2014 Drought impact on vegetation productivity in the Lower Mekong Basin. *Int. J. Remote Sens* 35, 2835–2856, 10.1080/01431161.2014.890298
- Ziv G , Baran E , Nam S , Rodríguez-Iturbe I , Levin SA , 2012 Trading-off fish biodiversity, food security, and hydropower in the Mekong River Basin. *P. Natl. Acad. Sci. USA* 109, 5609–5614, 10.1073/pnas.1201423109



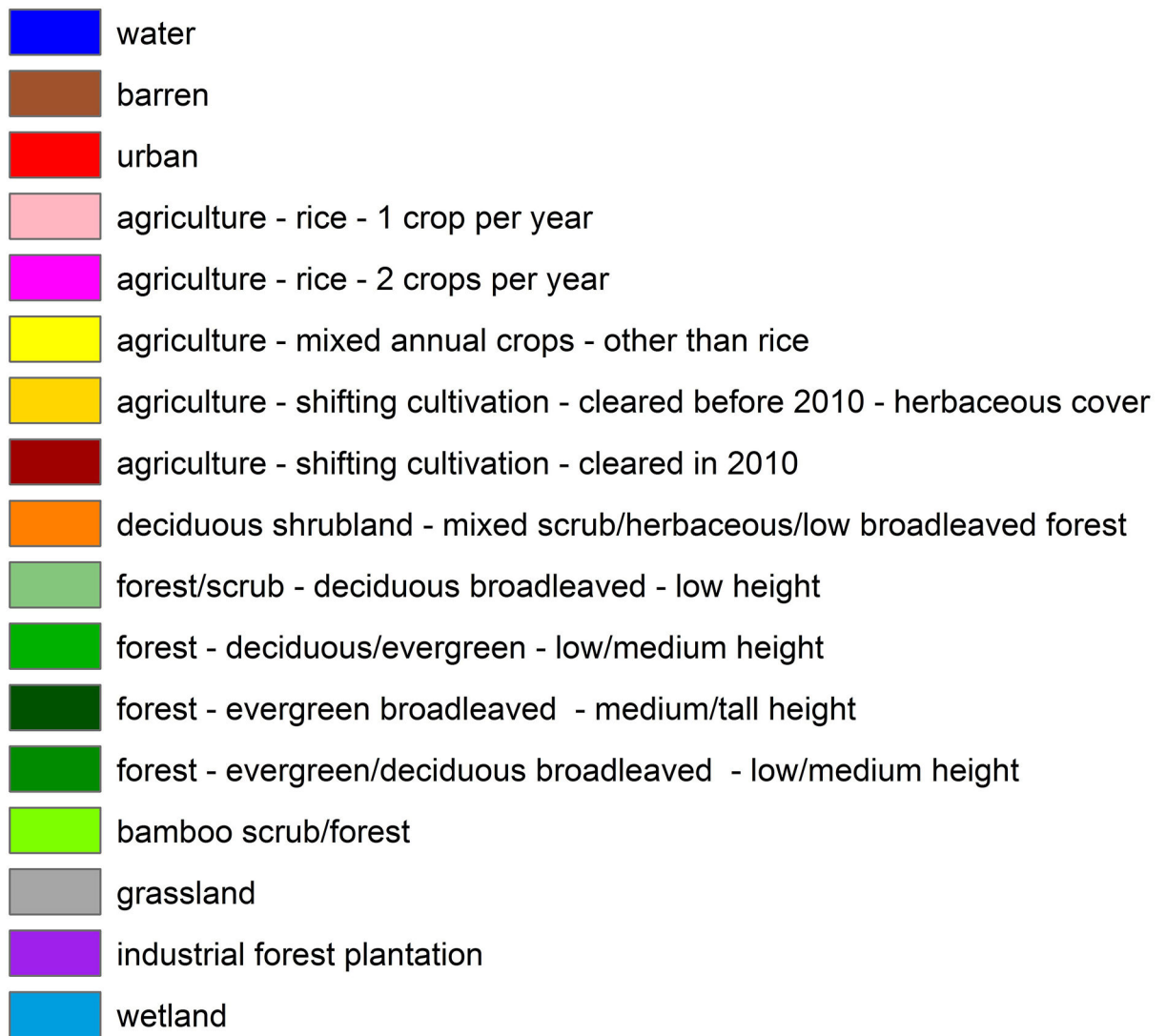


Figure 1.

The Lower Mekong River Basin. Streamflow gauges follow the Lower Mekong River Basin subareas presented by *Rossi et al.*, (2009). Cities with population classes obtained from Environmental Systems Research Institute, Inc. (ESRI) World Populated Places layer (<https://www.arcgis.com/home/index.html>, accessed on 31 May 2018) are depicted in red (greater than 5 million), orange (1–5 million), and light green (0.5–1 million). Land use and land cover class descriptions are given as a separate legend. Dam data are described in Appendix A.1.

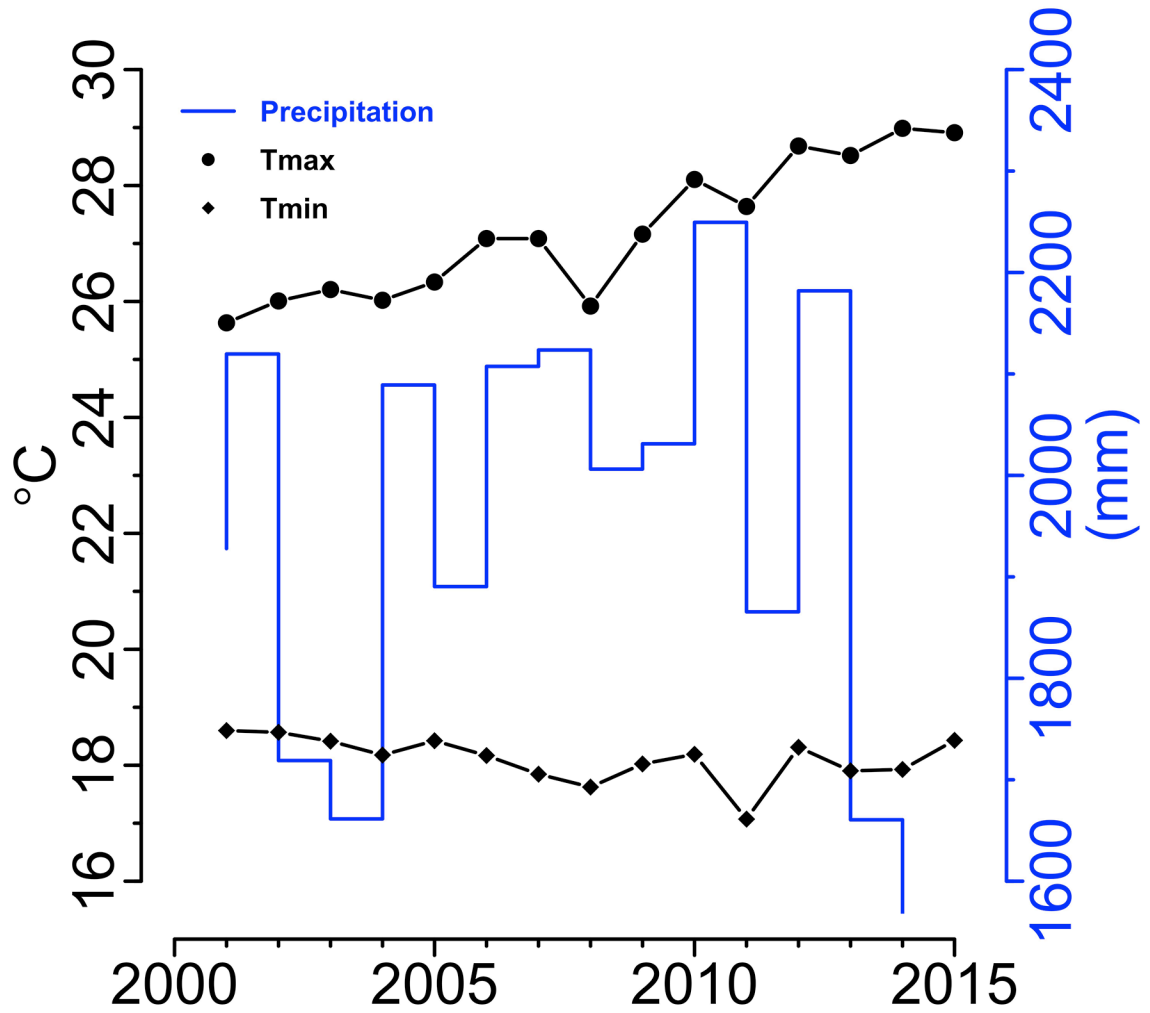


Figure 2. Lower Mekong basin time series data. Annual precipitation in millimeters (colored in blue), mean annual maximum air temperature (colored in black) in degrees Celsius, and mean annual minimum air temperature (colored in black) in degrees Celsius time series data are aggregated over the entire Lower Mekong basin.

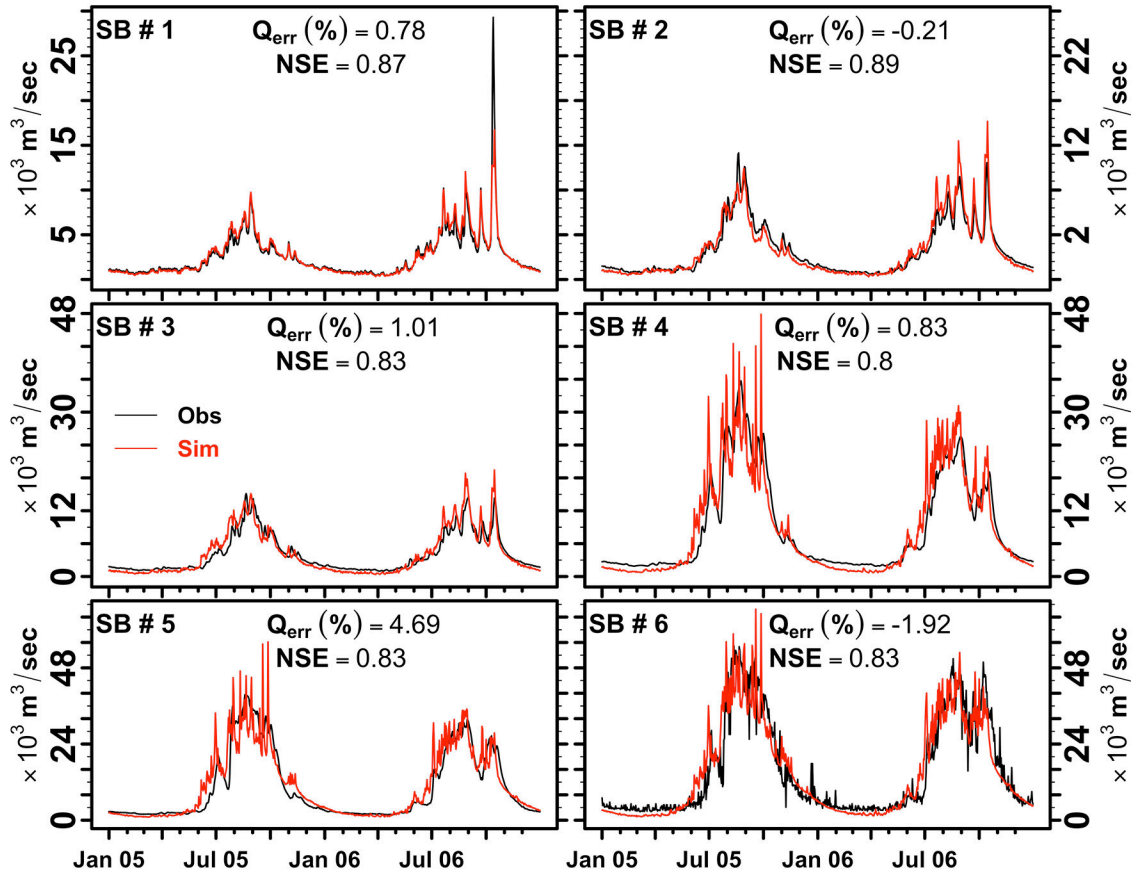


Figure 3. Daily simulated and observed discharge in m^3/sec for the Lower Mekong River at six sub-basin watersheds as presented in Figure 1 in calibration of the LMRB model. The LMRB model calibration years are 2005 and 2006. The percent error (Q_{err}) between daily simulated and observed discharge and the Nash–Sutcliffe (NSE) performance metrics are depicted for each sub-basin.

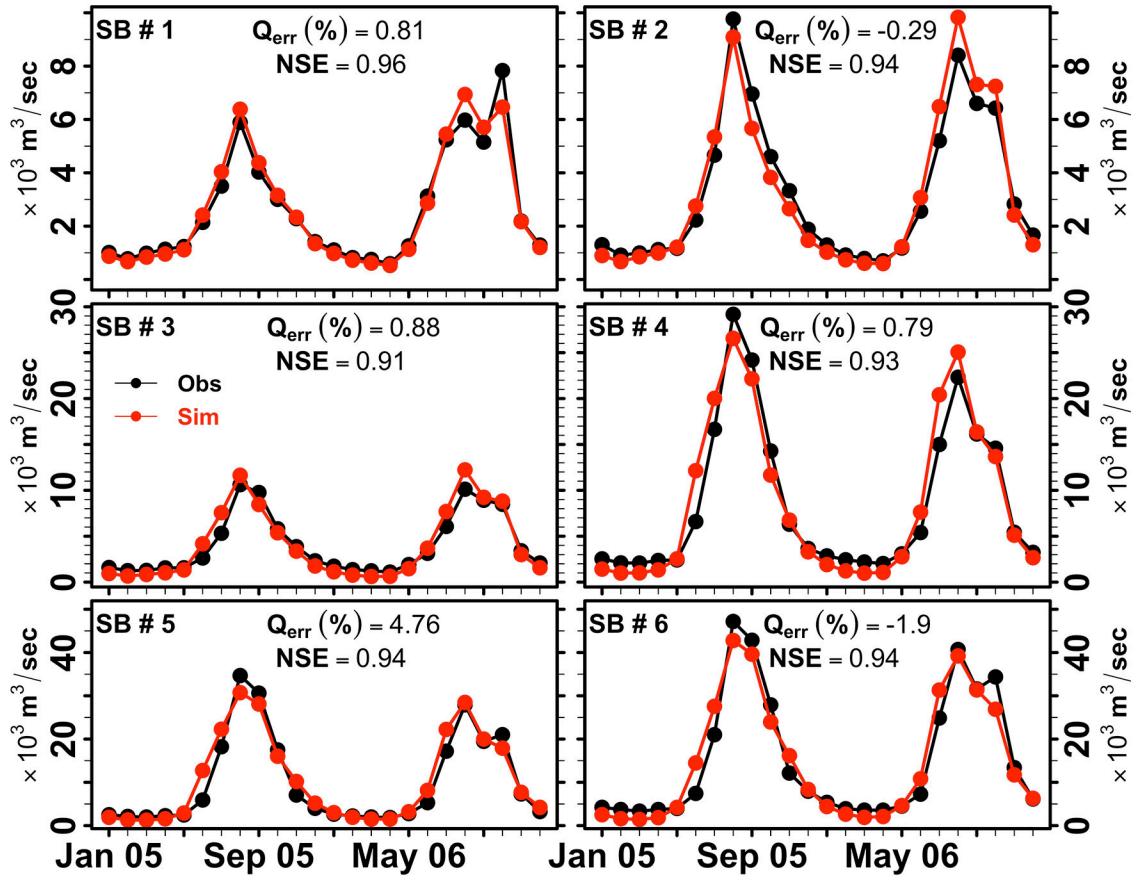


Figure 4. Monthly mean observed and simulated discharge (m^3/sec) for the Lower Mekong River at six sub-basin watersheds as presented in Figure 1 in calibration of the LMRB model. The LMRB model calibration years are 2005 and 2006. The percent error (Q_{err}) between monthly mean simulated and observed discharge and the Nash–Sutcliffe (NSE) performance metrics are depicted for each sub-basin.

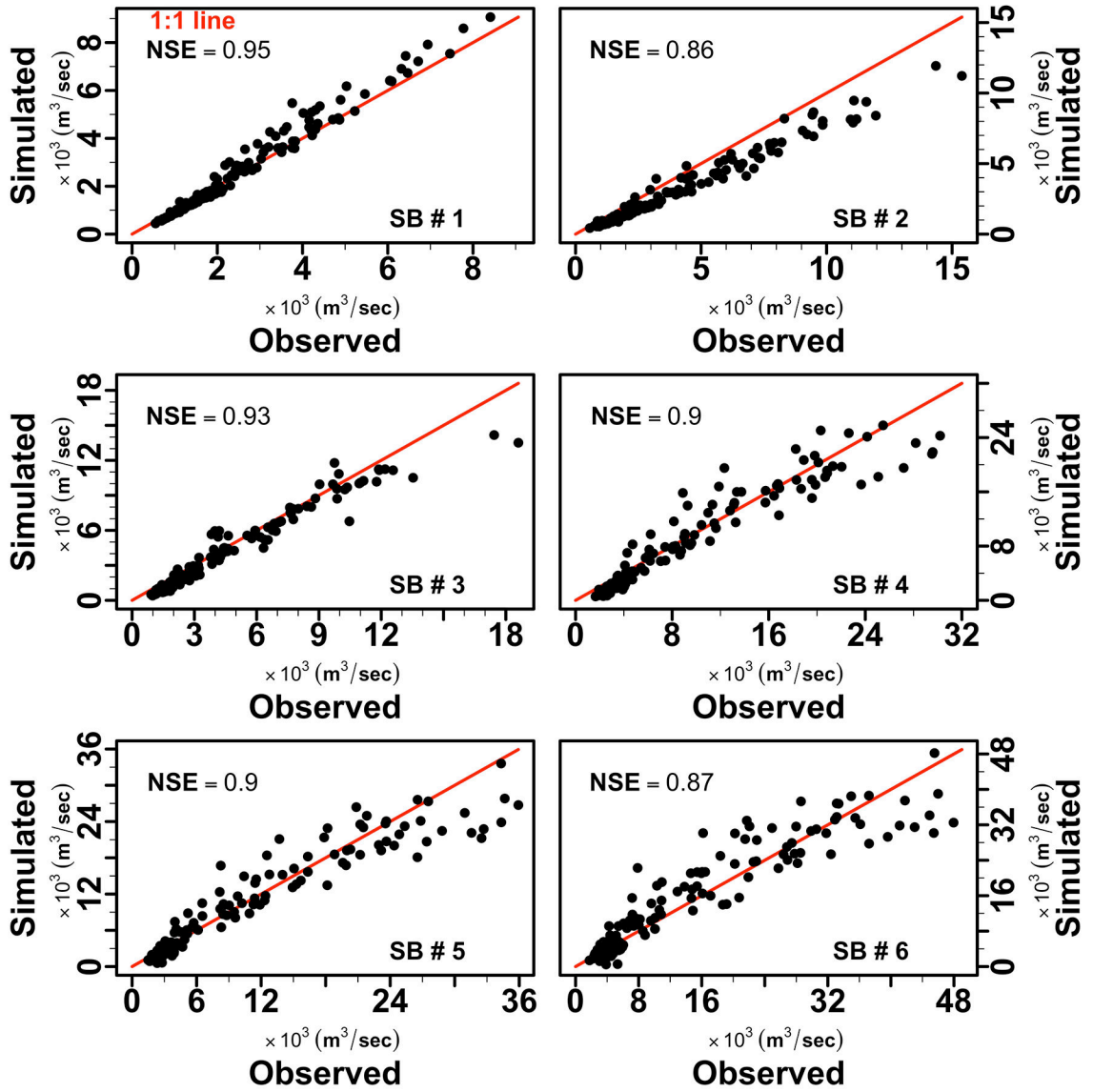


Figure 5. Scatterplot of monthly observed and simulated discharge in m^3/sec for the Lower Mekong River at six sub-basin watersheds in validation of the LMRB model during 2001–2004, and 2007–2015. The Nash–Sutcliffe (NSE) performance metrics during validation time period are depicted for each sub-basin.

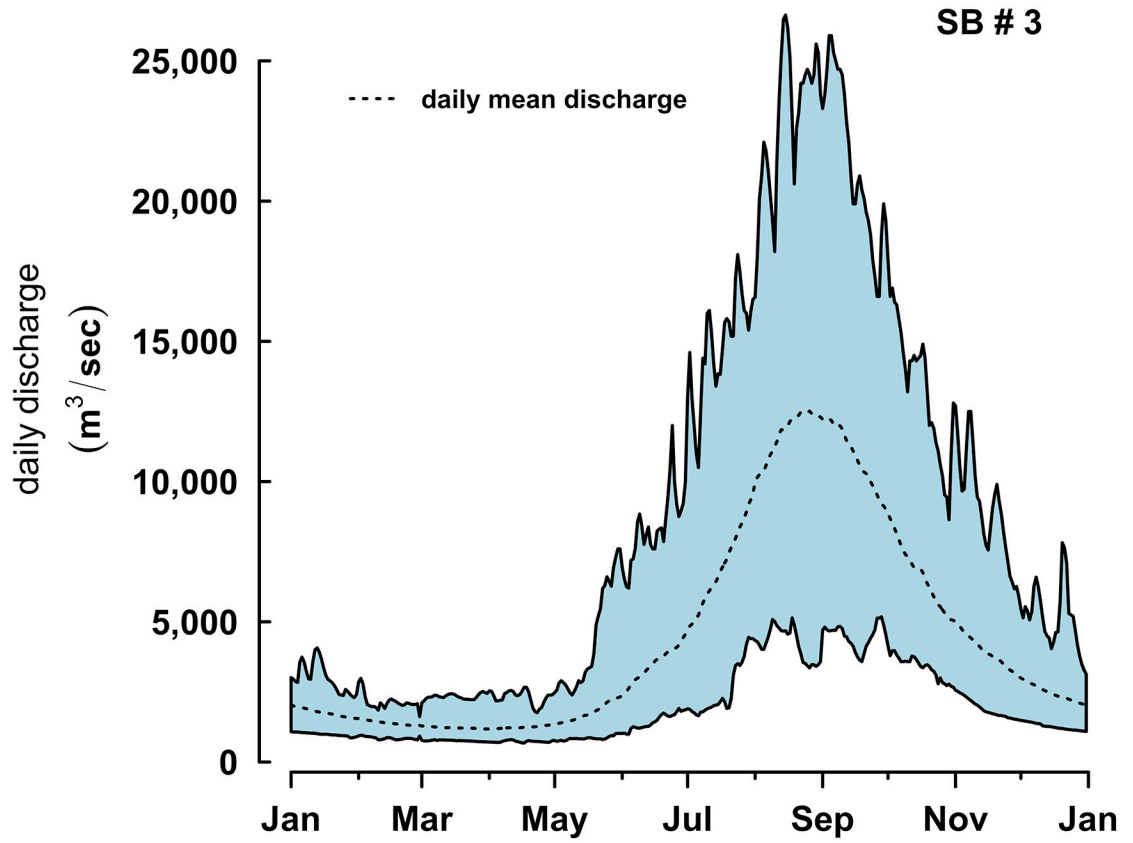


Figure 6. Vientiane (SB3) hydrograph. Mean, minimum, and maximum daily discharge during 1913–2016.

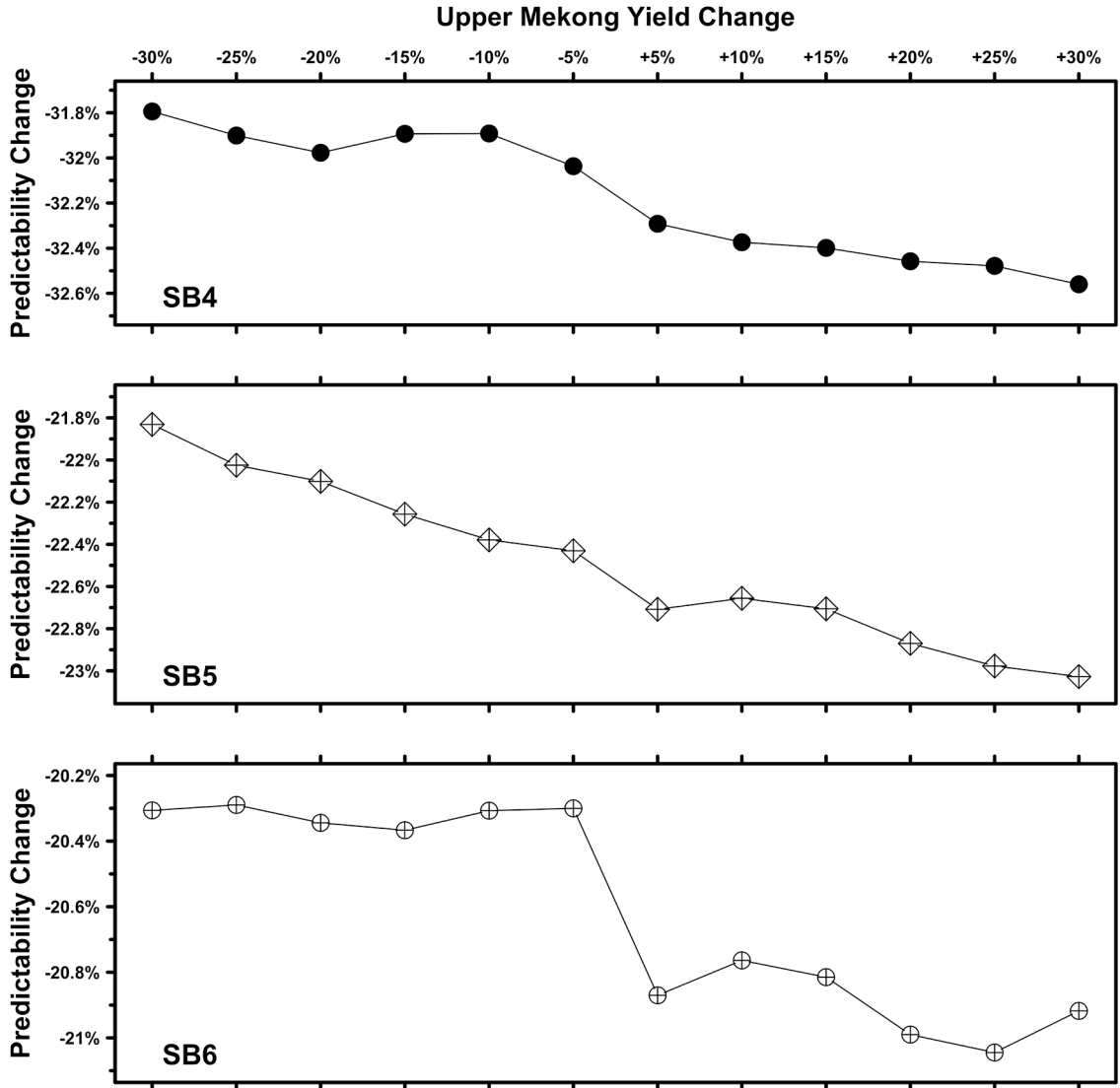


Figure 7. Sensitivity analysis for the Lower Mekong River Basin Colwell index predictability (P). Observed predictability during 2001–2015 time period at SB4, SB5, and SB6 is 0.342, 0.325, 0.317 respectively. Predictability change from observed predictability depicted in y-axis at each panel were calculated from simulated flow obtained by driving the LMRB model with adjusted Upper Mekong River flow inputs during the 2001–2015 time period as outlined in x-axis. Predictability change (y-axis) reports the scaled predictability change, i.e., $(P_{sim} - P_{obs})/P_{obs} \times 100$. Sub-basin watersheds follow description in Figure 1.

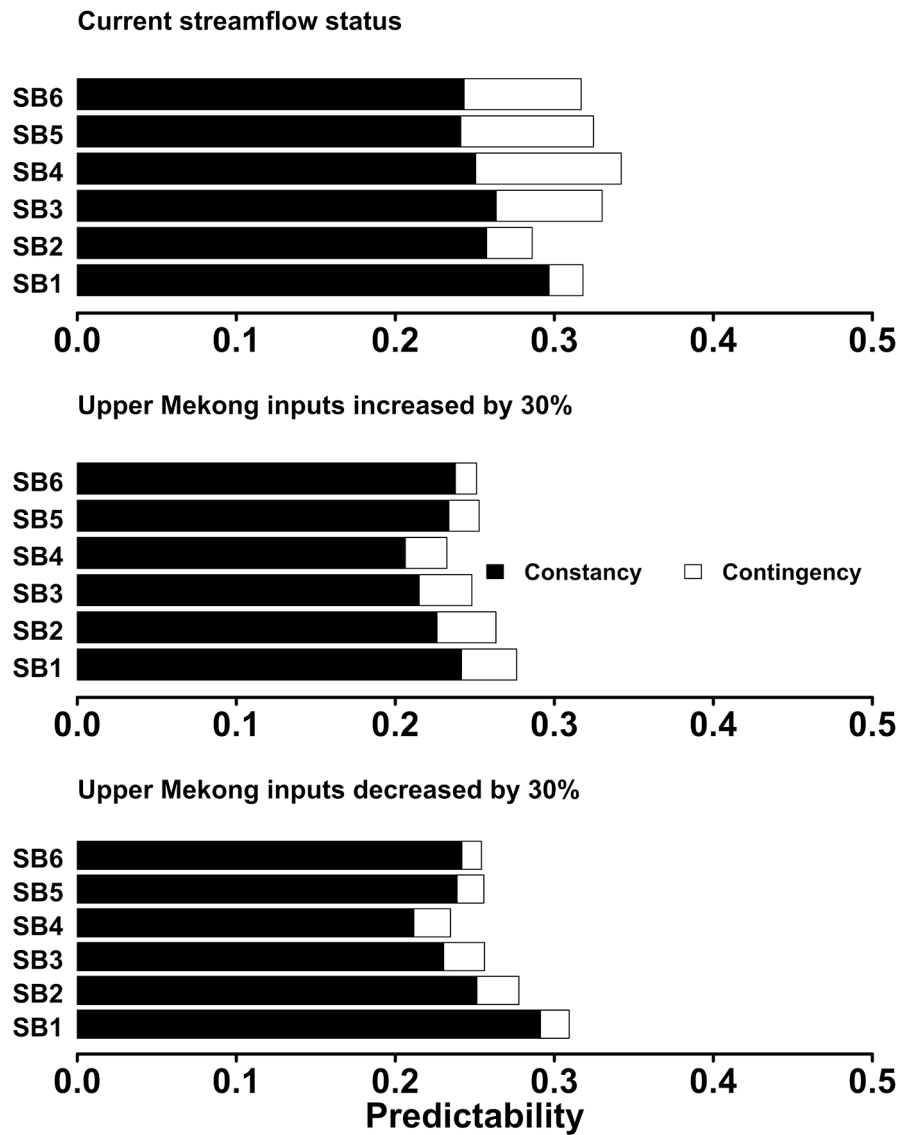


Figure 8. Colwell index, Predictability (P), Constancy (C), and Contingency (M) of streamflow for the Lower Mekong River Basin. Data for current streamflow status Colwell predictability analyses are daily discharge for the years 2001–2015. Flow simulations for different scenarios predictability analyses were obtained by driving the LMRB model with adjusted UMRB flow inputs during the 2001–2015 time period. Sub-basin watersheds follow description in Figure 1.

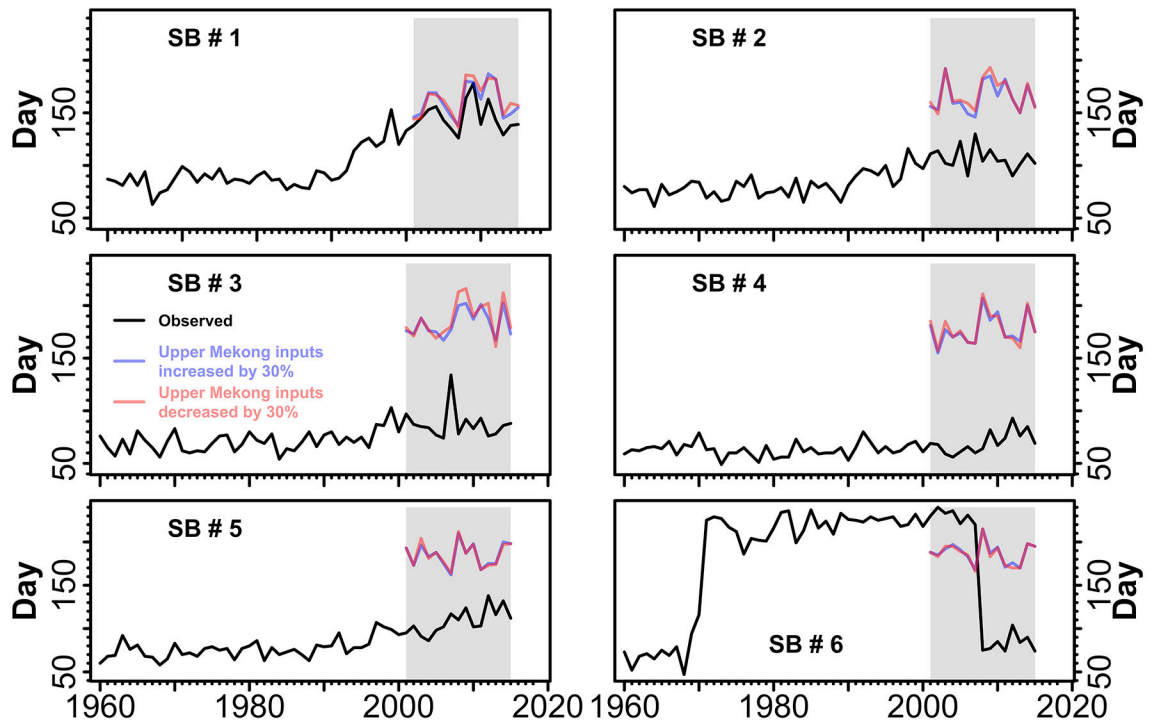


Figure 9. Annual flow reversal analyses at the LMRB. Black line gives flow reversals (*FLOWREV*) in days for the time period of 1960–2015 calculated from observed discharge, blue line gives (*FLOWREV*) calculated from simulated discharge with the UMRB inflow increased by 30%, and red line gives (*FLOWREV*) calculated from simulated discharge with the UMRB inflow decreased by 30%. Simulation discharge time period is 2001–2015 highlighted in grey. Sub-basin watersheds follow description in Figure 1.

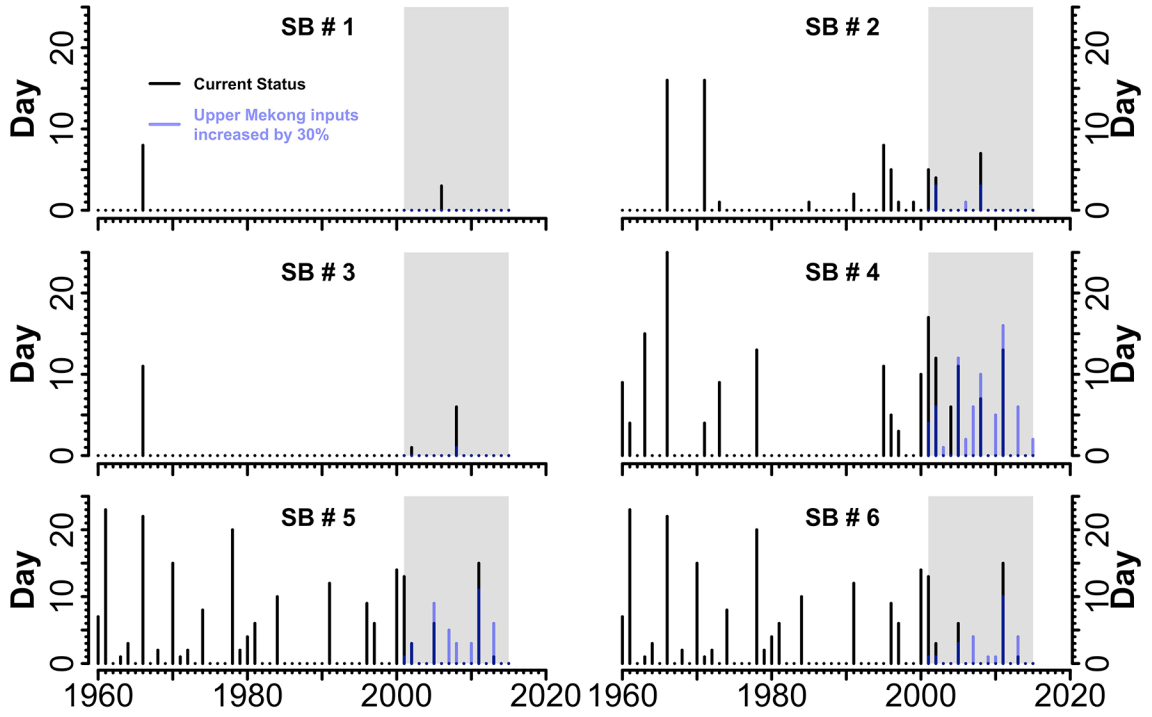


Figure 10. Flood duration (*FLDDUR*) analyses at the LMRB. The flood duration in days are the number of days when discharge equals or exceeds a threshold discharge magnitude causing floods. Black bars give flood duration in days for the 1960–2015 time period calculated from observed discharges, and blue bars give flood duration calculated from simulated discharges with the UMRB inflow increased by 30%. Simulation discharge time period is 2001–2015 highlighted in gray. Sub-basin watersheds follow description in Figure 1.

Table 1.

Streamflow regime variables used to assess the Lower Mekong flow changes.

| Variable name | Acronym | Definition | Streamflow classification |
|---------------------------------|----------------|---|-------------------------------------|
| Coefficient of variation | <i>DAYCV</i> | The ratio of the standard deviation of daily flows to the average of daily flows multiplied by 100 during a calendar year | Flow variability and predictability |
| Flow reversal | <i>FLOWREV</i> | The average number of daily flow reversals per year | |
| Colwell index of Predictability | <i>P</i> | Predictability of flow using an index developed by Colwell (1974) which is based on information theory | |
| Colwell index of Constancy | <i>C</i> | | |
| Colwell index of Contingency | <i>M</i> | | |
| Flood duration | <i>FLDDUR</i> | The average number of days per year when flow equals or exceeds <i>flood threshold</i> | High flow disturbance |
| 7 day maximum flow | <i>7QMAX</i> | The average annual maxima of 7 day means of daily mean streamflow | |

The Lower Mekong River annual discharge statistics. Discharge units are in m³/sec. Country codes are: CN (China), TH (Thailand), LA (Laos, PDR), and KH (Cambodia). The drainage area units are in square kilometers. The Q_{min} and Q_{max} refer to the minimum and the maximum annual discharge over the record at each site. The Q_1 , Q_2 , and Q_3 refer to the 25th, 50th (median), and 75th percentile of the mean annual discharge at each site. The μ refers to the mean annual discharge over the record, σ is the unbiased standard deviation, CV is the coefficient of variation, γ is the skewness, H is the Hurst coefficient (Hurst, 1951; Weron, 2002). The coefficient of variation CV is equal to σ/μ .

Table 2.

| Station Name | Code | Country | LMRB | Start Date | End Date | Drainage Area | Q_{min} | Q_1 | Q_2 | Q_3 | Q_{max} | μ | σ | CV | γ | H |
|----------------|--------|---------|--------------------|------------|------------|---------------|-----------|--------|--------|--------|-----------|--------|----------|------|----------|------|
| Chinese Border | 010000 | CN | Upper basin inlet | 1/1/1985 | 12/31/2007 | — | 1,619 | 2,010 | 2,157 | 2,459 | 2,763 | 2,221 | 303 | 0.14 | 0.03 | 0.35 |
| Chiang Sean | 010501 | TH | Sub-basin 1 outlet | 1/1/1960 | 12/31/2016 | 191,055 | 1,871 | 2,304 | 2,564 | 2,929 | 4,027 | 2,618 | 427 | 0.16 | 0.60 | 0.72 |
| Luang Prabang | 011201 | LA | Sub-basin 2 outlet | 1/1/1939 | 12/31/2016 | 273,838 | 1,852 | 3,410 | 3,754 | 4,177 | 5,488 | 3,777 | 707 | 0.19 | -0.12 | 0.70 |
| Vientiane | 011901 | LA | Sub-basin 3 outlet | 1/1/1913 | 12/31/2016 | 303,528 | 2,677 | 3,975 | 4,455 | 4,900 | 6,111 | 4,476 | 710 | 0.16 | 0.10 | 0.67 |
| Mukdahan | 013402 | TH | Sub-basin 4 outlet | 1/1/1923 | 12/31/2016 | 394,134 | 5,256 | 7,246 | 8,031 | 9,012 | 10,496 | 8,071 | 1,168 | 0.14 | -0.02 | 0.89 |
| Pakse | 013901 | LA | Sub-basin 5 outlet | 1/1/1923 | 12/31/2016 | 550,955 | 6,835 | 9,095 | 10,050 | 11,165 | 12,918 | 10,066 | 1,434 | 0.14 | -0.08 | 0.68 |
| Kratie | 014901 | KH | Sub-basin 6 outlet | 1/1/1924 | 12/31/2016 | 656,518 | 6,599 | 11,891 | 13,527 | 15,077 | 19,562 | 13,411 | 2,591 | 0.19 | -0.41 | 0.77 |
| Yasothon | 370104 | TH | Sub-basin 7 outlet | 1/1/1952 | 12/31/2003 | 46,805 | 77 | 171 | 240 | 287 | 602 | 242 | 102 | 0.42 | 1.21 | 0.60 |
| Rasi Salai | 380134 | TH | Sub-basin 8 outlet | 1/1/1979 | 12/31/2003 | 43,878 | 5 | 95 | 154 | 223 | 447 | 177 | 107 | 0.60 | 0.79 | 0.94 |

Table 3.

Parameters and calibrated values used for the LMRB model simulations. The identifier code refers to replace (V), addition (A), and multiplication (R).

| Parameter | Description | Range | Identifier code | Calibrated Value |
|---------------|--|--------------|-----------------|--------------------|
| Precipitation | | | | |
| High Flow | Correction factor to grid precipitation record | -1, +0.01 | R | -0.445 to +0.00225 |
| Base Flow | CN2 | -0.1, +0.1 | R | -0.07 |
| | AWC | -0.1, +0.1 | R | +0.07 |
| | ESCO | +0.5, +0.9 | V | +0.6 |
| | GWHT | 0, +1.0 | V | +0.075 |
| | GW_DELAY | -30, +60 | A | -14.25 |
| | GWQMN | -1000, +1000 | A | -450 |
| | REVAPMN | -750, +750 | A | +262.5 |
| GW_REVAP | Percolation to the deep aquifer to occur | +0.02, +0.10 | V | +0.042 |
| RCHRG_DP | Groundwater "revap" coefficient | | | |
| | Deep aquifer percolation fraction | -0.05, +0.05 | A | +0.0375 |

Table 4.

Annual DAYCV analyses at the LMRB during the 2001–2015 time period. The $DAYCV_{\mu}$ column is the arithmetic mean of the annual DAYCV in percent. Values in parentheses refer to mean annual DAYCV during the 1960–2015 time period. Sub-basin 7 and 8 streamflow time record is different than the rest of the Sub-basin streamflow record as listed in Table 2. UMRB input adjustment scenarios simulation discharge time period is 2001–2015. Country codes are similar to descriptions in Table 2.

| No. | LMRB | Station Name | Country | Code | $DAYCV_{\mu}$ |
|--|--------------------|---------------|---------|--------|---------------|
| 1 | Sub-basin 1 outlet | Chiang Sean | TH | 010501 | 70.10 (76.52) |
| 2 | Sub-basin 2 outlet | Luang Prabang | LA | 011201 | 80.73 (82.85) |
| 3 | Sub-basin 3 outlet | Vientiane | LA | 011901 | 81.83 (84.51) |
| 4 | Sub-basin 4 outlet | Mukdahan | TH | 013402 | 88.57 (93.56) |
| 5 | Sub-basin 5 outlet | Pakse | LA | 013901 | 95.38 (97.25) |
| 6 | Sub-basin 6 outlet | Kratie | KH | 014901 | 93.41 (95.68) |
| 7 | Sub-basin 7 outlet | Yasothon | TH | 370104 | (116.68) |
| 8 | Sub-basin 8 outlet | Rasi Salai | TH | 380134 | (154.31) |
| Inputs from Upper Mekong increased by 30% | | | | | |
| 1 | Sub-basin 1 outlet | Chiang Sean | TH | 010501 | 84.46 |
| 2 | Sub-basin 2 outlet | Luang Prabang | LA | 011201 | 90.89 |
| 3 | Sub-basin 3 outlet | Vientiane | LA | 011901 | 94.53 |
| 4 | Sub-basin 4 outlet | Mukdahan | TH | 013402 | 100.84 |
| 5 | Sub-basin 5 outlet | Pakse | LA | 013901 | 93.99 |
| 6 | Sub-basin 6 outlet | Kratie | KH | 014901 | 91.69 |
| 7 | Sub-basin 7 outlet | Yasothon | TH | 370104 | 84.48 |
| 8 | Sub-basin 8 outlet | Rasi Salai | TH | 380134 | 91.05 |
| Inputs from Upper Mekong decreased by 30% | | | | | |
| 1 | Sub-basin 1 outlet | Chiang Sean | TH | 010501 | 68.45 |
| 2 | Sub-basin 2 outlet | Luang Prabang | LA | 011201 | 78.90 |
| 3 | Sub-basin 3 outlet | Vientiane | LA | 011901 | 86.10 |
| 4 | Sub-basin 4 outlet | Mukdahan | TH | 013402 | 97.92 |
| 5 | Sub-basin 5 outlet | Pakse | LA | 013901 | 91.54 |
| 6 | Sub-basin 6 outlet | Kratie | KH | 014901 | 90.25 |
| 7 | Sub-basin 7 outlet | Yasothon | TH | 370104 | 84.48 |
| 8 | Sub-basin 8 outlet | Rasi Salai | TH | 380134 | 91.05 |

Seven-day maximum flow at the LMRB during 2001–2015 Mann Kendall trend analysis. The μ is the arithmetic mean of the seven-day maximum flow ($7QMAX$) in millimeter per day, τ (tau) is Kendall's tau correlation coefficient, p-value is 2 sided-test, and trend is Significant when ($p < 0.05$). Country codes are similar to descriptions in Table 2.

Table 5.

| LMRB Station Name | Sub-basin 1 outlet | Sub-basin 2 outlet | Sub-basin 3 outlet | Sub-basin 4 outlet | Sub-basin 5 outlet | Sub-basin 6 outlet |
|--|--------------------|---------------------|--------------------|--------------------|--------------------|--------------------|
| Country | Chiang Sean TH | Luang Prabang LA | Vientiane LA | Mukdahan TH | Pakse LA | Kratie KH |
| Code | 010501 | 011201 | 011901 | 013402 | 013901 | 014901 |
| μ | 3.3 | 3.8 | 4.0 | 6.1 | 5.3 | 6.0 |
| τ , tau | -0.486 | -0.219 | -0.410 | -0.314 | -0.333 | -0.352 |
| p-Value | 0.013 | 0.276 | 0.038 | 0.113 | 0.092 | 0.075 |
| Trend | Significant | No Trend | Significant | No Trend | No Trend | No Trend |
| Inputs from Upper Mekong increased by 30% | | | | | | |
| μ | 4.2 | 3.7 | 4.1 | 6.1 | 4.9 | 5.9 |
| τ , tau | -0.390 | -0.333 | -0.352 | -0.029 | -0.124 | -0.029 |
| p-Value | 0.048 | 0.092 | 0.075 | 0.921 | 0.553 | 0.921 |
| Trend | Significant | No Trend | No Trend | No Trend | No Trend | No Trend |
| Inputs from Upper Mekong decreased by 30% | | | | | | |
| μ | 2.8 | 2.7 | 3.2 | 5.5 | 4.5 | 5.5 |
| τ , tau | -0.314 | -0.219 | -0.200 | 0.048 | 0.067 | 0.105 |
| p-Value | 0.113 | 0.276 | 0.322 | 0.843 | 0.767 | 0.621 |
| Trend | No Trend | No Trend | No Trend | No Trend | No Trend | No Trend |

Table A. 1.

Dams data within the Mekong Basin obtained from CGIAR (WLE, 2017). Country codes are similar to descriptions in Table 2 with the addition of VN as Viet Nam. The COD column refers to the Commercial Operation Date (i.e. when the dam was commissioned).

| No | Name | Country | River | Latitude | Longitude | Function | Status | COD Year | Installed capacity Megawatts | Mean annual energy Gigawatts | Height meter | Crest length meter | Full supply level Million m ³ | Max reservoir area km ² | Est cost MILL \$ | Power destination (%) | | | | | | | Developer | Owner operator | Notes | | | | | | | | |
|----|---------------|---------|-------------|-------------|--------------|------------|--------------------|-------------|---------------------------------|---------------------------------|-----------------|-----------------------|---|---------------------------------------|---------------------|-----------------------|-----|-----|-----|-----|-----|-----|-----------|----------------|-------|-----|---|--|---|--|------------------------|--|---|
| | | | | | | | | | | | | | | | | LAO | THA | CAM | VN | CHN | MYN | IND | | | | | | | | | | | |
| 1 | Lower Sesan 2 | KH | Sa San | 13° 33' 5" | 106° 15' 50" | Hydropower | Under construction | 2019 | 480 | 2,311.8 | 4.5 | 7,729 | 1,790 | 335 | 781.52 | 0 | 0 | 30 | 70 | 0 | 0 | 0 | 0 | 0 | 0 | 0 | HydroLancang and Royal Group | EGL Gen (100%) | Location defined from Sesan, Sa San, and Sreng (Sb) River Basin Development Study in Kingdom of Cambodia, Lao People's Democratic Republic, and Socialist Republic of Viet Nam. ADB - RFA 4082. | | | | |
| 2 | Nam Ngum 1 | LA | Nam Ngum | 18° 31' 52" | 102° 32' 51" | Hydropower | Commissioned | 1971 | 149 | 1,006.00 | 75 | 468 | 4,700 | 370 | 97 | 80 | 0 | 0 | 0 | 0 | 0 | 0 | 0 | 0 | 0 | 0 | Nam Thon Power Co. (Thailand) 33% / GOL 25% | | | | | | |
| 3 | Nam Thon 2 | LA | Nam Thon | 17° 59' 50" | 104° 57' 8" | Hydropower | Commissioned | 2009 | 1075 | 5,936.00 | 48 | 325 | 3,500 | 450 | 1300 | 7 | 93 | 0 | 0 | 0 | 0 | 0 | 0 | 0 | 0 | 0 | 0 | Electricity Generating Authority of Thailand | | | | | |
| 4 | Sribhorn | TH | Lam Dam Noi | 15° 12' 23" | 103° 25' 45" | Hydropower | Commissioned | 1971 | 36 | 86.00 | 42 | 940 | 1,987 | 288 | | 0 | 100 | 0 | 0 | 0 | 0 | 0 | 0 | 0 | 0 | 0 | 0 | 0 | 0 | Electricity Generating Authority of Thailand | | | |
| 5 | Ubol Ratana | TH | Nam Pong | 16° 46' 31" | 102° 37' 6" | Hydropower | Commissioned | 1966 | 25.2 | 57.00 | 35.1 | 885 | 2,259 | 410 | | 0 | 100 | 0 | 0 | 0 | 0 | 0 | 0 | 0 | 0 | 0 | 0 | 0 | 0 | 0 | 0 | Electricity Generating Authority of Thailand | https://en.wikipedia.org/wiki/Ubol_Ratana_Dam |
| 6 | Dak N' Teng | VN | Dak N' Teng | 12° 11' 46" | 107° 55' 36" | Hydropower | Commissioned | 2011 | 13 | 52.80 | 31 | 31.5 | 25.49 | 323 | | n/a | n/a | n/a | n/a | n/a | n/a | n/a | n/a | n/a | n/a | n/a | n/a | n/a | n/a | n/a | Data provided by IWREP | | |